Particle Orbits in General Relativity: from Planetary Solar System to Black Hole Environment

Kirill Vankov

Particle Orbits in General Relativity: from Planetary Solar System to Black Hole Environment

Kirill Vankov

kirill.vankov@univ-grenoble-alpes.fr

updated on 2018-09-25

Abstract

This work is devoted mainly to General Relativity particle dynamics in the whole range of gravitational field strength in the GR academic framework. There is an opinion among the Physical community that the problem is fully studied and understood in all its mathematical and physical aspects, however, it is not true. The exact full solutions of the GR equation of particle motion in the whole range of fields have never been studied. It is shown that approximate solutions are not sufficient for understanding the problems at the deeper level and formulating the criterion of empirical testing of the Einstein's theory. As an example of the weak field problem, for the first time we study Einstein's Mercury perihelion advance in full details including exact solutions in terms of angular and temporal dynamic variables. Similarly, exact solutions were obtained for strong field problems. Both studies reveal some controversial issues, actually, known in literature but not paid sufficient attention, or remained physically unexplained, for example, a nonremovable singularity, the superluminal motion, solutions in terms of two dynamic temporal variables t and τ, and other issues. Consequently, we conduct an additional study of the particle dynamics in the alternative, the Special Relativity framework, with the conclusion that the GR controversial issues do not arise there. Overall, novel methodological and technical ideas and the corresponding results related to the whole range of field strength are claimed. The work is intended to stimulate further constructive discussions among researchers in Fundamental and Modern Physics, and Physics Frontiers, also, it has a pedagogical value.

Key words: GR dynamics; GR orbits classification; exact GR solution; special relativity dynamics

Contents

1 Introduction

1.1 Motivations and goals

The work is devoted mainly to General Relativity (GR) particle dynamics in the whole range of gravitational field strength. The study is conducted in the academic GR framework. This means that GR particle dynamics is defined by solutions of Einstein's equation of motion [1] without any additional assumptions and physical properties usually introduced in Astrophysical models of orbital motions. The ideal model of the test particle motion in the spherical symmetric geometry is used.

As an example of the weak field problem, Einstein's Mercury perihelion advance is studied. There is a wide opinion among the Physical community that the problem is fully studied and understood in all its mathematical and physical aspects. This opinion is supported by "mainstream" workers and mass media, actually, causing a scientific stagnation. In reality, such an opinion is not true. The exact full solutions of the GR equation of motion, particularly, describing temporal dependent orbital radius $r(\theta)$ and $r(\tau)$ have never been studied. Instead, the approximate field models and solutions were used. However, the errors due to approximations and assumptions cannot be assessed without the knowledge of exact solutions. Nowadays, when mathematical high precision and effective computational methods are available, consistent formulations of relativistic dynamics problems and their full exact reproducible solutions need to be studied and understood at a new deeper level.

There are numerous works, in which Einstein's General Relativity and, particularly, his explanation of Mercury's anomaly is criticized for allegedly erroneous derivation of the GR effect. Most of those works come from non-qualified authors having no sufficient research experience. However, there are a significant number of GR experts who challenge Einstein's work by suggesting its "modifications" or "corrections", such as Modified Newtonian Dynamics (MOND), and others.

A recent *disagreement* example is the work by Engelhard [2]. In mass media, it initiated a vivid exchange of opinions, as well as comments, discussions, criticism, suggestions from all categories of specialists, including top experts in the field. The author relates Einstein's prediction of the Mercury anomaly to the previously derived Gerber's formula. Though, it is identical

to Einstein's one, it is based on very different assumptions proven wrong (no matter if Einstein was aware or not of this work at that time). Yet, the author put Einstein's prediction in connections with the GR radial fall formula and suggested to use a physical solution for free fall obtained by taking into account the dependence of mass on velocity in Newton's gravitational law. We consider this multi-aspect work not relevant to Einstein's Dynamics and destructing the readers' attention from the basic principle of GR methodology.

In our work, we study exact angular and temporal solutions to Einstein's original GR Dynamics equation [1] in the whole range of field strength. As a result, it is found that the GR prediction of perihelion angular advance for *the weak field*, apart from the corresponding GR temporal shift with respect to the classical picture, is not sufficient for understanding Gravitational Relativistic Dynamics of at the deeper level, in particular, the problem of formulating the criteria of empirical testing of Einstein's theory.

While conducting the study, we also pay a close attention to the controversial issues in GR problems of particle motion in both weak and strong fields, and those regardless of field strength. They are actually known in literature, but mostly ignored in GR expertise literature, or still remained unresolved problems and controversies. To some of them we return in the text, for example, the incompatibility of Special Relativity (SR) with physical gravity phenomenon, the central and "removal" infinities, existence of two dynamic time variables, τ and t, the particle spiral fall, the causality violation in superluminal motion, and others.

In view of such issues, we additionally study Relativistic Particle Dynamics in the alternative, SR based framework, on the same footing as in GR framework. The conclusion is made that no controversies or inherent contradictions arise there, and solutions are self-consistent.

Overall, we state that the work contains novel methodological and technical ideas and results concerning the GR Dynamics and relevant Physical branches, which are outlined throughout the text. The novelties include

- the exact full solutions of GR dynamics equations in the whole range of gravitational field strength,
- the formulation of comparison criteria needed for empirical tests of theoretical predictions,
- evaluations of precision requirements in computations and observations,

- similar studies in the alternative SR framework, and related methodological and technical novelties.

The work must be interesting to numerous open-minded readers, first of all, among Physical Community and workers in Fundamental and Modern Physics, including Astronomy, Astrophysics, Cosmology, and relativistic gravity.

1.2 Historical review of Einstein's problem in brief

We consider the GR historical development essential for understanding of the current status of relativistic particle dynamics, therefore, its brief historical review is presented here.

Originally, Einstein's derivation of the non-classical effect in Mercury's orbit was based on some assumptions and approximations, among which, weak field conditions in the scheme of "a perturbation of the classical equation" [1]. Most of responding publications of different authors on the subject were modifications of Einstein's methodology of particle dynamics, see reviews in [3, 4, 5]. A special attention deserves the work by Hagihara [6] (1931). He published a monograph about the application of the theory of elliptic functions for deriving exact analytic solution of Einstein's problem, in particular, concerning the Mercury's perihelion anomaly. The predicted GR effects must be seen as a very small deviation from the classical theory. Obviously, technical level of computations at that time was too low to realize the method in practice, so the results were of qualitative interest.

Later on, Chandrasekhar [7] (1983) studied the problem analytically in terms of elliptic function solution in relationship with the GR Black Hole (BH) concept. However, he modified original Einstein's equation in order to obtain a simplified numerical solution in terms of classical geometrical parameter, "an effective eccentricity", in combination with effective physical parameters. Consequently, the solution deviated from the exact one, the difference having not being evaluated, that made difficult to reveal GR non-classical aspects of space-time curvature. The GR Mercury problem was not studied.

Recently, Kraniotis and Whitehouse [8] (2003) used the theory of elliptic functions to obtain the exact solution in order to reproduce Einstein's GR prediction of Mercury's anomaly. Even before their publication, there was a wide belief among Physics community that the above Einstein's problem had been fully studied. In reality, in the work the exact angular solution to the

Mercury's problem was realized for the first time. However, conditions of arbitrary field strength, the time-dependent problems, and criteria of comparison of GR versus Newtonian predictions were not studied there. More historical references can be found in [3].

Over time, the treatment of the problem has changed after finding the Schwarzschild metric being an exact solution to Einstein's field equations. Consequently, the original Einstein's equation of particle motion nowadays is considered valid in the whole range of field strength. It allow us to study weak field GR effects and strong-field phenomena on the same footing, for example, hypothetical super-massive Black Holes.

2 The GR particle dynamics

2.1 The GR equation of particle dynamics

The equation of GR particle dynamics in a spherical symmetric geometry (usually, in polar coordinates) was originally presented by Einstein in [1] more than hundred years ago

$$\left(\frac{\mathrm{d}x}{\mathrm{d}\theta}\right)^2 = \frac{2\,A}{B^2} + \frac{\alpha}{B^2}x - x^2 + \alpha\,x^3\,, \tag{1}$$

where $x = 1/r$ is the inverted radius; A and B are the total energy and the angular momentum, correspondingly; $\alpha = 2\,r_g = 2\,G\,M/c^2$ is the Schwarzschild radius, r_g is called the gravitational radius. Here, the mass of gravitational field source M is however greater than the mass of the orbiting body, $M \gg m$, the latter body is considered the standard test particle.

In the contemporary presentation, the equation explicitly includes the term of particle proper mass/energy (that is, the rest mass); the classical components of the total energy are summed up quadratically. The cubic GR term makes the equation principally different from the corresponding classical equation. Under the weak field conditions, the term of potential energy in the dimensionless form is as small as $r_g/r_0 \ll 1$, where r_0 is the distance of the test particle from the gravitational source, the speed of light is usually taken $c = 1$.

With the field strength, the GR effects drastically rise, and the test particle can reach the speed close to the speed of light. Under spiral fall conditions, it

exceeds the speed of light what is interpreted in terms of superluminal motion.

It should be noted that there is some similarity between formal solutions in the GR and Classical theories: in both, the test particle can reach the speed of light at the Schwarzschild radius, however, the Classical theory, unlike GR, is considered valid only in the restricted weak field range. Unlike in GR, the spiral fall cannot happen in Classical theory.

2.2 The Lagrangian solution, and the formulation of initial conditions

There are several approaches to how to derive the equation in the contemporary presentation. Kraniotis and Whitehouse [8] present a review on how it comes from Einstein field equations with the use of Christoffel symbols under conditions of spherical symmetry. Alternatively, it is derived from the Schwarzschild metric [9, 10].

A more quick way is based on the Hamiltonian Action Principle S with the Lagrangian L in analogy to classical mechanics [11]

$$\delta S = \delta \int_{t_1}^{t_2} L(q_i, \dot{q}_i, t)\, \mathrm{d}t = 0\,, \tag{2}$$

where q_i and $\dot{q}_i$ are generalized coordinates and their time derivatives $\dot{q}_i = \partial q_i/\partial t$ characterizing the system, $i = 1, 2, \ldots, N$. The Lagrangian is chosen with the idea to find the extremal path between the starting and ending points in the variational integral S:

$$\frac{\partial L}{\partial q_i} - \frac{\mathrm{d}}{\mathrm{d}t}\frac{\partial L}{\partial \dot{q}_i} = 0\,. \tag{3}$$

In General Relativity, the Lagrangian describing the test particle motion is usually taken in the form $L = \mathrm{d}\tau/\mathrm{d}t$, see [11]. It is obtained from the Schwarzschild metric, where $\mathrm{d}s = c\,\mathrm{d}\tau$ is the world line element, τ is the proper time, and t is the coordinate time. The metric in the quadratic form with the signature $[+,\ -,\ -,\ -]$ is given by

$$\mathrm{d}\tau^2 = (1 - 2\,r_g/r)\,\mathrm{d}t^2 - (1 - 2\,r_g/r)^{-1}\,\mathrm{d}r^2 - r^2\,\mathrm{d}\theta^2\,, \tag{4}$$

where the speed of light and the particle mass are taken $c = 1$, $m = 1$.

The Lagrangian is

$$
\begin{aligned}
|L| &= \mathrm{d}\tau/\mathrm{d}t \\
&= \left((1-2\,r_g/r) - (1-2\,r_g/r)^{-1}(\mathrm{d}r/\mathrm{d}t)^2 - r^2\,(\mathrm{d}\theta/\mathrm{d}t)^2\right)^{1/2}\,,
\end{aligned}
\tag{5}
$$

where $q_1 = r$ and $q_2 = \theta$.

Two constants of motion follow from the consideration of the ignorable temporal and angular variables. First, the conserved angular momentum is $l_0 = r\,(\mathrm{d}\theta/\mathrm{d}\tau)$. Second, the conserved total energy comes out from the Hamiltonian

$$
H = \sum_i \dot{q}_i \frac{\partial L}{\partial \dot{q}_i} - L\,. \tag{6}
$$

When $l_0 = r\,(\mathrm{d}\theta/\mathrm{d}\tau) = 0$, the conserved energy (in a dimensionless form) can be found

$$
\epsilon_{rad} = (1-2\,r_g/r)\,\mathrm{d}t/\mathrm{d}\tau\,. \tag{7}
$$

The subscript (rad) there stands for the total energy in the particular case of pure radial motion when $l_0^2 = 0$. The corresponding equation of the radial motion is discussed later.

It should be immediately noted that, for a motion with the angular momentum $l_0 \neq 0$, the equations of motion are necessarily derived in terms of temporal dynamic variable τ, which determines the GR metric form (4) and plays there a role of the abstract proper time. One can expect that the equations of motion are formulated in the observable coordinate system with the coordinate time t. The latter is supposedly present in expressions of metric and the following Lagrangian. We return to this problem later.

Let us set the initial conditions at an apsis $r = r_0$: let it be $\theta_0 = 0$, the angular component of the velocity $\beta_\theta = \beta_0 \neq 0$, the radial speed component $\beta_r(r_0) = 0$, recall that the speed of light here is $c = 1$, and the test particle mass $m_0 = 1$. Then, a dimensionless parameter $\rho_0 = r_g/r_0$ characterizes the potential field strength. There is one more degree of freedom allowing to reduce dimensional parameters to dimensionless ones, namely, we can define the initial radius $r_0 = 1$ and return to its physically real value in the final results to be compared with observations. Next, let us introduce a dimensionless variable, the inverted radius, $\xi = r_0/r$, $\xi_0 = 1$.

There must be three roots ξ_i in the GR cubic equation of motion, one of them can be fixed $\xi_0 = 1$, therefore, two other roots can be given by simple

algebraic expressions, that is, in terms of elementary functions. This is our technical novelty, which is tremendously helpful in obtaining the exact solutions of equations of motion. Actually, two and only two of any independent parameters (not necessarily roots) will determine the unique solution for a given initial conditions. Once an appropriate set of independent parameters is specified, the connection between any pair of them can be established. A pair of two independent parameters could be, for example, ρ_0 and β_0^2 specified at the periapsis (or apoapsis), or some their independent combination like ρ_0 and $\sigma_0 = \rho_0/\beta_0^2$.

To sum up, we have a set of desired equations of motions in the dimensionless form, in which dimensionless parameters are connected with the physical quantities determining the initial conditions $\rho_0 = r_g/r_0$, β_0^2 (in the dimensionless form). They are also related to the conserved total energy $\epsilon_0 = \epsilon(\xi)$ and other quantities (among them, the effective potential $V_{eff}(\xi)$), which are explicit functions of ξ: V_{eff}^2, β_r^2, β_θ^2, $\beta^2 = \beta_r^2 + \beta_\theta^2$. The conserved squared angular momentum is found in the form $l_0^2 = r_0^2\,\beta_0^2 = \beta_\theta^2/\xi^2$ (here $\beta_\theta = r\,\mathrm{d}r/\mathrm{d}\tau$). There are other interconnected equations

$$\begin{aligned} \epsilon_0^2 &= 1 - 2\,\rho_0 + \beta_0^2 - 2\,\rho_0\,\beta_0^2 \\ &= 1 - 2\,\rho_0\,\xi + \beta_0^2\,\xi^2 - 2\,\rho_0\,\beta_0^2\,\xi^3 + \beta_r^2(\xi)\,, \end{aligned} \tag{8}$$

and from this

$$\begin{aligned} \beta_r^2(\xi) &= \epsilon_0^2 - 1 + 2\,\rho_0\,\xi - \beta_0^2\,\xi^2 + 2\,\rho_0\,\beta_0^2\,\xi^3 \\ &= \beta_0^2 - 2\,\rho_0 - 2\,\rho_0\,\beta_0^2 + 2\,\rho_0\,\xi - \beta_0^2\,\xi^2 + 2\,\rho_0\,\beta_0^2\,\xi^3\,, \end{aligned} \tag{9}$$

$$\beta_\theta^2(\xi) = (r_0\beta_0)^2\,\xi^2\,, \tag{10}$$

$$\beta^2(\xi) = \beta_r^2(\xi) + \beta_\theta^2(\xi)\,, \tag{11}$$

$$V_{eff}^2(\xi) = \epsilon_0^2 - \beta_r^2(\xi)\,. \tag{12}$$

From the equality $\mathrm{d}\xi/\mathrm{d}\theta = \beta_r(\xi)/\beta_0$ easily proved, the equation of motion $\mathrm{d}\xi/\mathrm{d}\theta = f(\xi)$ follows:

$$\left(\frac{\mathrm{d}\xi}{\mathrm{d}\theta}\right)^2 = \left(1 - \frac{2\,\rho_0}{\beta_0^2} - 2\,\rho_0\right) + \frac{2\,\rho_0}{\beta_0^2}\,\xi - \xi^2 + 2\,\rho_0\,\xi^3\,. \tag{13}$$

2.3 The GR τ versus t and other problems of the two theories comparison

As noted above, the GR Dynamics equations of motion with non-zero angular momentum are derived from the quadratic metric form $\mathrm{d}\tau^2$ appearing to be defined in the abstract proper space-time (4). However, the corresponding GR equations respect conserved total energy and angular momentum, consequently, the time variable τ serves the role of a dynamic variable in the observable coordinate space-time. The 4-coordinates are functions of τ, correspondingly, their derivatives are taken with respect to the time variable τ too but not the coordinate time t, as should be.

This is the known controversial issue related to the interpretation of GR theoretical framework. It was acknowledged by Einstein and later on by other GR researchers. In practice, τ is often interpreted in terms of the comoving observer in the coordinate space, otherwise, it is replaced by t on the premises of weak-field conditions. Bearing this controversy in mind, one can think that GR Dynamics equations are reduced to the classical ones by dropping the GR cubic term in (13) and its corresponding parts in the initial conditions.

However, there are more problems of the two theories comparison, – one of them is the use of the ideal model, in which a point particle of mass m rotates about a central attractor of mass M in spherical symmetric geometry. The particle is considered the test particle that is, its mass is required to be however small $m \ll M$ in the one-body problem. This is true in both GR and Classical theories. We shall see, however, that GR Dynamics, unlike Newtonian Dynamics, does not admit the N-body problem (even for N=2). One has to conclude that GR equations cannot be *consistently* reduced to the corresponding classical equations, as discussed further in more details.

2.4 The GR Newtonian limit

The classical Keplerian equation for $r(\theta)$ is the one-body problem solvable analytically in terms of one-parameter elementary function. The unique solution takes the dimensionless form [3]

$$\theta(\xi) = \int \frac{\mathrm{d}\xi}{\sqrt{(1-2\,\sigma) + 2\,\sigma\,\xi - \xi^2}}\,, \tag{14}$$

therefore

$$\xi(\theta) = \xi_0 \, (\sigma_0 - (1 - \sigma_0) \cos\theta) \, . \tag{15}$$

Recall, the dimensionless form comes with physical constants of test particle mass $m_0 = 1$ and the speed of light $c = 1$, and the space-time normalization is taken by $r_0 = 1$.

The quantity $\sigma = r_g/(r_0\beta_0^2)$ absorbs the initial condition data $r = r_0$, $\beta_r = 0$, $\beta_\theta = \beta_0$, $\theta = \theta_0 = 0$ and serves as the σ_0 criteria of classification of all possible orbits in Classical Mechanics, bounded and unbounded.

The initial angle is fixed $\theta_0 = 0$ that leaves 3 variable physical parameters (r_g, r_0, β_0) to characterize orbit families with *absolute* orbit sizes, time motion and speeds (say, in meters, seconds, and masses kg. One can find connections between geometrical and physical parameters. In the classical equation of motion and its unique solution in the dimensionless form, the only one, necessary and sufficient, parameter σ is needed. The orbit type is determined by a value of σ-parameter, see illustration in fig. 1.

The σ-classification of classical orbits	
$0 < \sigma < 0.5$	hyperbola
$\sigma = 0.5$	parabola
$0.5 < \sigma < 1$	overcircle ellipse
$\sigma = 1$	circle
$1 < \sigma < \infty$	subcircle ellipse

The above (physical) classification of a family of orbits is advantageously different from the conventional (geometrical) one. A family of orbits with a variable eccentricity e and a fixed semi-latus rectum p are not suitable for our analysis. The parameter σ imposes a physically consistent constraint on a classical family of orbits. As a result, a remarkable σ-gauge symmetry of particle dynamics in a spherical symmetric gravitational field takes place: any change of initial data (r_g, r_0, β_0, or equivalently r_g, r_0, l_0^2) preserving σ_0 does not change the character of the particle motion.

Notice, in geometrical 2-parameter representation, there is no such categories as sub and over circle orbits. Besides, the classical dynamics becomes invalid as the field strength rises. The GR phenomenon such as a spiral fall of the test particle onto the center does not appear there. This makes the comparison of the two theories complicated.

The σ_0 parameter also relates to the Virial Theorem in terms of an averaging potential and kinetic energies over time periods. This theorem can be principally generalized in relativistic theories dealing with *unclosed* orbits. Our strong recommendation to Astronomers is to use the σ_0 classification of orbits instead of traditional two physically correlated geometrical parameters.

There is, in our view, the fundamentally wrong statement often made in GR textbooks with respect to the reduction of GR Dynamics to Newtonian gravitation under the assumptions of low speed and weak field (discussed in [12]). It states that Newton's universal law in a general case of arbitrarily distributed matter over the space follows from Einstein's field equations (in some analogy to Electrostatics). The Poisson equation is meant

$$\Delta\phi = 4\pi G\mu\,. \tag{16}$$

where μ is the mass distribution. The key concepts in this claim is the potential $\phi(\vec{R})$, and the related potential energy U. Here $R = \sqrt{(X_1^2 + X_2^2 + X_3^2)}$, – the magnitude of the radius vector pointed from the coordinate origin in 3-space. Consider the particular case of mass distribution, – a ball of mass m and the potential about it

$$\phi = -\frac{Gm}{R} \tag{17}$$

and, consequently, the force $F = -m'\partial\phi/\partial R$ acting in this field on another ball of mass m'

$$F = -\frac{Gmm'}{R^2}\,. \tag{18}$$

This is the well known Newton's law of attraction, but its derivation from the GR theory is flawed for the following reason. The classical concept and definition of potential assume that *another ball of mass m' is the test particle* not disturbing the field that is, its mass is however small $m' \ll m$.

There is a fundamental cause for the GR theory being not reducible to the corresponding classical theory. It is rooted in properties of Einstein's field equations (EFE). One can draw this conclusion from the detailed physical analysis of the solutions discussed in GR textbooks. Firstly, the τ vs t conflict in both GR Dynamics and Statics originates in the EFE. Secondly, the equations admit only two types of solutions necessarily defined in the whole infinite 3-space. We are interested in the type of vacuum solutions (zero Ricci tensor). Solutions of the second type (the medium filled with continuously distributed mass, non-zero Ricci tensor) are used in cosmological theories and

it is not relevant to our problem.

The intermediate case, when finite massive matter is present in the form of gravitationally interacting pieces, is theoretically admitted in the Classical theory. The corresponding solution of the Poisson equation (16) can be formulated as the N-body problem. However, this case is impossible in Einstein's theory of gravitational field [13]. Newtons attraction law (18) is a 2-body problem but there could not be any GR analogy or "GR reduction" to it. The GR Mercury problem is necessarily one-body problem that is, the planet is considered the point test particle with the mass however small in comparison with the Solar mass. The correction for the mass finiteness is not legitimate there.

Surprisingly, the GR cubic term in GR Dynamics results in a huge complexity of non-classical solutions and difficulties of the two theories comparison. In the concluding part of the work, the comparison criteria in relationship with empirical tests of theoretical predictions are formulated.

3 Classification of the GR orbits

3.1 Analytic connections between parameters of the motion equation and cubic roots

The advantageous form of our presentation of the GR equation of motion (13) is that it is dimensionless and scaled to the initial condition $\xi_0 = 1$, and as such, it is governed by only two independent physical parameters fixed in the initial conditions. In the integral form, the exact unique solution is given by

$$\theta(\xi) = \int \frac{\mathrm{d}\xi}{\sqrt{\left(1 - \frac{2\,\rho_0}{\beta_0^2} - 2\,\rho_0\right) + \frac{2\,\rho_0}{\beta_0^2}\,\xi - \xi^2 + 2\,\rho_0\,\xi^3}}\,, \tag{19}$$

where integration is performed within the range between the first root $\xi_1 = \xi_0 = 1$ and the second root ξ_2 if it is real or to infinity. It could be one or three real roots ξ_1, ξ_2, ξ_3. Among three roots of the polynomial, any pair of them are physically independent.

In Einstein's problem, physical constraints are imposed on the equation, first of all, the conservations laws. Additional constraints come from the variable rescaling. The dimensionless form of equations with the first root

$\xi_1 = \xi_0 = 1$ allows us to easily determine other two roots without using Tartaglia and Cardano formulas for the roots of a cubic and then make a unique physical classification of solutions.

Let

$$f(\xi) = 2\,\rho_0\,\xi^3 - \xi^2 + \frac{2\,\rho_0}{\beta_0^2}\,\xi + \left(1 - \frac{2\,\rho_0}{\beta_0^2} - 2\,\rho_0\right)\,, \tag{20}$$

then

$$\frac{f(\xi)}{\xi - 1} = 2\,\rho_0\,\xi^2 - (2\,\rho_0 - 1)\,\xi - \left(1 - \frac{2\,\rho_0}{\beta_0^2} - 2\,\rho_0\right) \tag{21}$$

is a quadratic polynomial in ξ with a simple expression for its roots:

$$\xi_{2,3} = \frac{1 - 2\,\rho_0 \pm \sqrt{1 + 4\,\rho_0 - 12\,\rho_0^2 - 16\,\rho_0^2/\beta_0^2}}{4\,\rho_0}\,. \tag{22}$$

3.2 Types of GR orbits in terms of roots

The Lagrangian problem formulation implies that all GR trajectories are periodic and time reversal, as in classical mechanic. However, while in classical mechanics the angular period is always $2\,\pi$, in GR the angular period takes larger values dependent on initial conditions. The GR perihelion advance effect is valid for any type of GR orbits including unbounded ones.

From the expression (8) for the total energy in the settings of the equation (13), it follows that a condition $\epsilon_0 \geqslant 1$ requires that $\beta_0^2 \geqslant 2\,\rho_0/(1 - 2\,\rho_0)$. For this condition $\epsilon_0 \geqslant 1$, up to $\rho_0 \leqslant 1/4$, the trajectories are all unbounded: either parabolic or hyperbolic. However, for $\rho_0 > 1/4$ and $2\,\rho_0/(1 - 2\,\rho_0) \leqslant \beta_0^2 < \rho_0/(1 - 3\,\rho_0)$, the total energy ϵ_0 is greater or equals to 1, but the trajectory of a particle is of a spiral fall type, i.e. the motion is bounded.

All possible variants of roots are shown in fig. 2. There are several cases when types of orbits depend, firstly, on the roots being real or complex, secondly, on specific values of ξ_2 and ξ_3. The integration of the equation (19) is performed from the first root $\xi_1 = 1$ over the positive part of $f(\xi)$ to the next root or up to the infinity, see example in section 4.2. There are special cases $\xi_2 = \xi_3$, $\xi_2 = 0$, $\xi_2 = 1$, and $\xi_3 = 1$, for which one needs to find the explicit relationships between ρ_0 and β_0^2 corresponding to three curves on (ρ_0, β_0^2) plane. These curves divide the plane into four regions with a specific trajectory type. Six types of trajectories are possible: hyperbola, parabola, circle, over-circular precessing ellipse, sub-circular precessing ellipse, and spiral fall to the center, see table 1 and fig. 3.

The regions of the classical orbits in β_0^2 vs ρ_0 plane are shown in fig. 4. While the first root is fixed, $\xi_1 = 1$, the second root is $\xi_2 = 2\,\sigma - 1$ (recall, $r = 1/\xi$). therefore, unbounded motion appears for ξ crossing zero value and going into negative side. The case, when $\xi_2 = 0$, that is when $\sigma = 1/2$, corresponds to a parabolic orbit. The case, when $\xi_2 < 0$, that is when $\sigma < 1/2$, corresponds to a hyperbolic orbit. The other values of σ correspond to elliptic orbits. In particular, for $\sigma = 1$ one has $\xi_2 = 1$, which corresponds to a circular orbit. This picture can be compared with the analogous GR one, see fig. 3.

Notice that types of orbits, which are similar in GR and classical mechanics, have different regions in (ρ_0, β_0^2) diagrams, this is also seen from a comparison of their parameters:

type of orbit	classical mechanics	general relativity
circular	$\beta_0^2 = \rho_0$	$\beta_0^2 = \dfrac{\rho_0}{(1-3\,\rho_0)}$, $\rho_0 \leqslant \frac{1}{4}$
parabolic	$\beta_0^2 = 2\,\rho_0$	$\beta_0^2 = \dfrac{2\,\rho_0}{(1-2\,\rho_0)}$, $\rho_0 < \frac{1}{2}$

It is also seen that in GR a new type of orbits exists, which we call a spiral fall trajectory, it is discussed later. This type of orbits does not exists in classical mechanics. It is characterized a particle fall on the center under specific conditions. In literature, it is associated with strong fields in the Black Hole environments.

4 Analytic and Numerical Solutions

4.1 Elliptic function method

The equation (19) can be recognized as an elliptic integral of the first kind (see any textbook on elliptic functions and elliptic integrals, for example, [14, 15]). It can be solved by means of the Weierstrass elliptic function $\wp$ [14, §20.6].

The $\wp$-function satisfies the following differential equation

$$(\wp'(z))^2 = 4\,(\wp(z))^3 - g_2\,\wp(z) - g_3\,, \tag{23}$$

where parameters g_2 and g_3 are known as the elliptic invariants. Conversely, given the equation

$$\left(\frac{\partial u}{\partial z}\right)^2 = 4\,u^3 - g_2\,u - g_3\,, \tag{24}$$

One gets the general solution

$$u = \wp(\pm z + \alpha)\,, \tag{25}$$

where α is the constant of integration. The equation $y^2 = 4\,x^3 - g_2\,x - g_3$ is known as the Weierstrass normal form of an elliptic curve. Therefore, the equation (13) can be solved in terms of the Weierstrass elliptic function $\wp$. Moreover, the solution can be given in a convenient form $r(\theta)$.

This approach is known, the following are just a few related articles that employed the Weierstrass elliptic function: Hagihara suggested classification of the trajectories in a gravitational field of Schwarzschild [6], Kraniotis and Whitehouse studied the perihelion precession of the orbit of the planet Mercury around the Sun [8], Lämmerzahl discussed the experimental basis of General Relativity [16].

In order to determine the corresponding parameters for $\wp$-function and the expression for the solution of (13), it is necessary to transform our equation into Weierstrass normal form. There are several ways to do this.

Consider the following linear substitution

$$\xi = \frac{2}{\rho_0}\,x + \frac{1}{6\,\rho_0}\,. \tag{26}$$

The equation (13) becomes

$$\left(\frac{\partial x}{\partial \theta}\right)^2 = 4x^3 - \left(\frac{1}{12} - \frac{\rho_0^2}{\beta_0^2}\right)x - \left(\frac{1}{216} - \frac{1+3\beta_0^2}{12\,\beta_0^2}\,\rho_0^2 + \frac{1+\beta_0^2}{2\,\beta_0^2}\,\rho_0^3\right)\,, \tag{27}$$

that is

$$\begin{aligned} g_2 &= \frac{1}{12} - \frac{\rho_0^2}{\beta_0^2}\,, \\ g_3 &= \frac{1}{216} - \frac{1+3\,\beta_0^2}{12\,\beta_0^2}\,\rho_0^2 + \frac{1+\beta_0^2}{2\,\beta_0^2}\,\rho_0^3\,. \end{aligned} \tag{28}$$

Therefore,

$$r(\theta) = \frac{6\,\rho_0\,r_0}{12\,\wp(\theta+\alpha; g_2, g_3) + 1}\,. \tag{29}$$

From the theory of Complex Analysis, it follows that the function $\wp$ is a meromorphic function in the complex plane. It is doubly periodic with two linearly independent periods $2\,\omega_1$ and $2\,\omega_2$. When the roots of the cubic $4\,x^3 - g_2 x - g_3$ are all real, one of the periods is purely imaginary, and another

is real. The real period corresponds to the angular period of motion described by the equation (13).

The function $\wp$ is a complex-valued function, however along the line $\alpha+\theta$, where orbital angle θ varies, the imaginary part of it vanishes. The value $\wp(\alpha) = (6\,\rho_0 - 1)/12$ corresponds to the initial condition $(r = r_0, \theta = 0)$ and equals to one of the roots of the cubic polynomial (27). This is the property of the function $\wp$ that values $\wp(\omega_1)$, $\wp(\omega_2)$ and $\wp(-\omega_1-\omega_2)$ are all three roots of the cubic. Therefore, the value of α is either ω_1, or ω_2, or $-\omega_1 - \omega_2$.

Algorithms for computing the periods for the case of real coefficients may be found in literature, see, for example, [17, Algorithm 7.4.8] or [18, §3.7]. The use of the real arithmetic–geometric mean allow one to compute both values rapidly with a high degree of precision. The theory of this method is described in [19]. It has been generalized in [20] allowing for complex-valued coefficients.

In practice, the software packages produce the corresponding $\wp$-function and compute the periods without requiring a user to transform the equation into the Weierstrass form. Most major mathematical software systems support computation with elliptic functions. We have chosen to use SAGE [21] because it is freely available, highly flexible and very efficient. Calculations can be performed with arbitrary precession, we used precision of 600 significant digits here. Moreover, the computations in SAGE can be performed on-line at `http://cocalc.com` without requiring a user to install software on a personal computer. SAGE also provides access to numerous other open source scientific packages, in particular, we used PARI/GP [22].

4.2 Numerical integration

Recall the integral form of the GR equation of motion (19). As in the above analytical solution, there are several singular cases where the integral does not converge. Depending on values of two parameters ρ_0 and β_0, the integration (19) is performed from $\xi_1 = 1$ to either ξ_2 or ξ_3.

Numerical integration procedure in PARI/GP takes into account the asymptotic behavior of integrating function at end points and compute the result with chosen arbitrary precision. Our direct integration numerical solution is in complete agreement with the solution produced using Weierstrass $\wp$-function.

As an example, consider a case when the cubic has three real roots, e.g. $\rho_0 = 0.05$, $\beta_0 = 0.04$. Then, the cubic polynomial in the equation (19)

becomes

$$f(\xi) = 0.1\,\xi^3 - \xi^2 + 2.5\,\xi - 1.6\,, \tag{30}$$

with roots $\xi_1 = 1$, $\xi_2 \approx 2.44$ and $\xi_3 \approx 6.56$, see fig. 6. The initial condition dictates the starting point $r_0 = 1/\xi = 1$, $\theta_0 = 0$, the integration (19) is performed from $\xi = 1$ to $\xi = \xi_2$:

$$\theta(\xi) = \int_1^{\xi_2} \frac{\mathrm{d}\xi}{\sqrt{0.1\,\xi^3 - \xi^2 + 2.5\,\xi - 1.6}}\,. \tag{31}$$

The full integral from 1 to ξ_2 corresponds to the periapsis position $r_p = 1/\xi_2 \approx 0.41$, $\theta_p = \int_1^{\xi_2} 1/\sqrt{f(x)}\,\mathrm{d}\xi \approx 4.53$, which is the closest approach to the central mass. From this point, the test particle motion continues in counter-clock direction. At the apoapsis point $r_a = r_0 = 1$, $\theta_a = 2\,\theta_p \approx 9.07$, the particle completes the first period, see fig. 7.

4.3 Time dependent exact solution

The time dependent problem in both Newtonian and GR mechanics can be solved only by numerical integration. In GR, the time dependent equation of motion, for example, follows from (9), where $\beta_r(\xi) = \mathrm{d}r/\mathrm{d}\tau$. Therefore,

$$\tau(\xi) = -\int \frac{\mathrm{d}\xi}{\beta_0\,\xi^2 \sqrt{\left(1 - \dfrac{2\,\rho_0}{\beta_0^2} - 2\,\rho_0\right) + \dfrac{2\,\rho_0}{\beta_0^2}\,\xi - \xi^2 + 2\,\rho_0\,\xi^3}}\,. \tag{32}$$

The integrand is exactly the same as in (19), and integration is performed along the same ξ interval. The expression (32) corresponds to the elliptic integral of the third type. In contrast to the case of the elliptic integral of the first type, there is no analytical expression similar to (29). Nevertheless, the theory of Complex Analysis implies that the solution $r(\tau)$ exists, and it is periodic. For practical purpose, we compute the integral (32) numerically.

5 GR Mercury's problem

5.1 The law $\Delta\theta = 3\,\sigma_{gr}\,\rho_0$ in the weak field

Knowledge of exact solutions of Einstein's problem allows us to quantitatively define weak field conditions and assess errors in approximate predictions. Let

us consider first the approximate value of the GR perihelion advance $\Delta\theta$ under the weak field conditions $\rho_0 \ll 1$ and compare it with the exact numerical results.

We suggest the following formula, precision of which increases when the field strength decreases so that in the limit $\rho_0 \to 0$ its computational error becomes however small.

$$\Delta\theta = 3\,\sigma_{gr}\,\rho_0\,, \tag{33}$$

Here, $\Delta\theta = \theta_{gr}/\theta_{cl} - 1$ is a relative angular shift rad/rad averaged over half a period, $\theta_{cl} = \pi$, $\sigma_{gr} = \sigma_0/(1 - 3\,\rho_0)$, actually $\sigma_{gr} = \sigma_0 = \rho_0/\beta_0^2$ for $\rho_0 \ll 1$. For Mercury ($\sigma_0 \approx 0.829457$), the calculated effect is exact to the precision, at least, 6 significant figures or 14 decimal places.

The law (33) is illustrated in fig. 8. The plotted data are positive angular deviations from π in %. There are two plots: the line for $\rho_0 = 0.001$ (a weak field), and the curve for $\rho_0 = 0.05$ (a mildly strong field). The line demonstrates the law (33) in the whole range of bounded motion. At $\rho_0 = 0.001$, the angular relative shift is 0.300% at $\sigma_{gr} = 1$.

For $\rho_0 > 0.050$, the GR effect is not linear with σ_{gr} anymore because of the field strength growing with σ_{gr}. For convenience of comparison, the normalization coefficient is selected $k = 1$ for $\rho_0 = 0.01$, so that $k = 10$ for $\rho_0 = 0.001$, and $k = 1/5$ for $\rho_0 = 0.05$. For $\rho_0 = 0.05$ the law is not good in the region of the sub-circle motion $\sigma_{gr} > 1$ and partly in the over-circle region $\sigma_{gr} > 0.7$.

Einstein claimed in [1] that his equation can explain the perihelion precession of the planet Mercury. Kraniotis and Whitehouse discussed in [8] this GR effect in greater details and showed the range of free parameters for which astronomer's observations are consistent with the GR theory prediction. In particularly they looked for "the best fit of input data" having the Solar mass and the conserved total energy fixed, and the conserved angular momentum varied. However, those parameters are physically correlated and contain more than two independent ones while Einstein's equation has the unique one solution characterized by the two and only two independent sufficient parameters, as shown in our analysis. Also, it is shown there that the equation in Mercury's case is highly sensitive to numerical precisions and rounding errors, especially with the usage of Tartaglia and Cardano formulas in [8]. To ensure stable numerical computations, we use the exact algebraic (dimensionless) solutions for roots in elementary functions.

5.2 The necessity of exact solutions of GR particle dynamics in space and time for GR observational tests

The test of GR prediction of Mercury's perihelion angular advance is the only one of classical GR tests, involving a material body. The relative difference between the GR angular period and the classical one of 2π was evaluated long ago and reevaluated many times later in the perturbation approach. This evaluation was made using an ideal model of undisturbed orbit in the weak field approximation resulting extremely small value, namely, 8.0×10^{-8} rad/rad, or $2\pi \times 8.0 \times 10^{-8}$ rad/revolution, which is hard to observe.

There is a historically neglected problem, though. It is related to the fact that the angular phase shift does not fully characterize the GR effect without the corresponding effect in the time period T. It is unfortunate that the time dependent problem $r(t)$, has never been studied before. The Mercury's orbit is the same one in angular and time scales, and both angular and temporal effects must be subjected to the empirical tests on the same footing.

Astronomers working in observations and their treatments, want theoreticians to provide them with numerical information serving as a chart of the object's trajectories in space and time, $r(\theta)$ with $\theta(t)$. The required information also includes values of the integral observables, which are predicted by GR and Classical theories. It must be given in the output databases, while a common set of initial data being evaluated from the current Astronomical observations constitutes the input database. Both will serve as the guidance for conducting new differential and integral observations made to the precision sufficient for *empirical* testing of theoretical predictions in the GR compared to the Classical Theory.

In particular, one needs to calculate values of angular and time periods and the corresponding differences in terms of angular and temporal shifts with respect to classical values. This should be a special program of "the empirical verification/falsification of Einstein's theory", in which the predicted data were compared with empirical high-precision tests. Putting such a statement, we challenge the widely spread, in our opinion, wrong belief that Einstein's prediction of the perihelion advance is thoroughly confirmed in numerous observations with no questions left.

In reality, the problem is even more complicated because the observations

are conducted under severe perturbation conditions due to N-body interactions of planets so that perturbation effects to be accounted for in treatments of observations are much greater than the relativistic effects. In such circumstances, the measurements of angular and temporal shifts require high precision techniques of observations of orbits in space and time, which were not available decades ago, and are probably not sufficient yet to meet the requirements. The N-body problem is out of the scope of this work. Here, we focus our attention on an exactly calculated orbit described in terms of both angular and time variables in the ideal conditions.

5.3 Einstein's perturbative approach and the GR approximate models

As an example of time variable involvement, consider the Mercury problem and the well known value there of angular GR advance $\Delta\theta_{cen}$ accumulated for Earth's 100 years (about 415 orbital evolution). Assuming the equivalence of GR and classical time periods, it would be $\Delta\theta_{cen} = 43$ arcsec. This number for the first time was obtained by Einstein in his perturbation method. He used the approximate estimate of the perihelion advance $\Delta\theta$ from his original equation (1). The value of $\Delta\theta_{cen}$ was claimed to be verified in contemporary theoretical works with the use of Einstein's methodology, see [23, 11, 24].

More specific, Einstein [1] started with the approximate estimate of the perihelion advance $\Delta\theta$ from his original equation (1) with $\alpha = 2\,r_g$, and geometrical parameters a - the semi-major axis, p - the semilatus rectum, e - eccentricity

$$\Delta\theta = 2\,\pi\,\frac{3\,\alpha}{2\,p} \tag{34}$$

and connected it with the classical time period T_{cl}

$$T_{cl} = \left(\frac{8\,\pi^2\,a^3}{c^2\,\alpha}\right)^{1/2} \tag{35}$$

It follows

$$\Delta\theta = \frac{24\,\pi^3\,a^2}{T_{cl}^2\,c^2\,(1-e^2)}\,. \tag{36}$$

This connection between $\Delta\theta$ and T_{cl} is a formal, because they are calculated in different theories independently, their full physical comparison is not conducted. Without the exact GR solution of the time dependent problem along

with the similar angular calculations, a physical intuition does not tell us if T_{gr} can be somehow greater or less than or equal to the corresponding classical value T_{cl}. To avoid an ambiguity in interpretations of the observational tests aimed to verify the theoretical predictions, one needs the full exact solution of the GR problem.

Besides Einstein's perturbation methodology, there are different approximate ways, in which evaluations of the angular shift is made with an involvement of the time variable. One way is to modify the classical orbit $r(\theta)$ to the form yielding the desired perihelion advance $\Delta\theta$ under the assumptions of a nearly circular uniform motion of the test particle in a weak field. To describe the orbital precession analytically in elementary functions, the parameter ν is introduced in a modified classical solution taken in the traditional geometric form of two parameters.

$$\xi(\theta) \approx (1/p)(1 + e\cos\nu\theta), \qquad r(\theta) \approx \frac{p}{(1 + e\cos\nu\theta)} \tag{37}$$

where $\xi = r_0/r$, $r_0 = 1$, and the angular precession is uniform. The quantity ν characterizes a cyclic frequency related to the angular frequency $\omega = 2\pi$ per revolution, meaning the classical time period of one revolution T_{cl} for $\nu = 1$.

The quantity $\nu \approx (1 - 3r_g/p) < 1$ is a new (third) parameter. A small correction $3r_g/p$ to the angular cyclic frequency should be interpreted as a factor of slowing down of the rotational motion in comparison with the analogous classical motion $\nu = 1$. Having $\nu < 1$, one has to think that, starting from the initial condition $r = r_0$ at $\theta = 0$, the radius would retake its initial value upon a completion of the GR period if the planet had to rotate through the additional angle $2\pi(3r_g/p)$ (the perihelion advance), in accordance with (37). For $\nu > 1$, it will be a retardation.

The above formula for GR angular advance is supposed to be a solution of the classical equation of motion modified by a change of variable $\theta \to \nu\theta$. The formula is thought to be an approximate GR solution, if the cubic term in the following corresponding GR equation is neglected:

$$\left(\frac{1}{\nu^2}\right)\left(\frac{dx}{d\theta}\right)^2 = -\frac{(1 - e^2)}{p^2} + \frac{2x}{p} - x^2 + 2r_g x^3\,. \tag{38}$$

In our view, this is not acceptable because the GR effect is due to the GR cubic term, hence, it cannot be neglected. In those approximations, the conservation laws are broken, and a determination of the time period of rotation becomes

ambiguous, hence, the above model is inherently contradictory.

In literature, they discussed another way, in which a similar model is suggested but, paradoxically, under the assumption that the angular motion speed is greater (but not less) than the speed of a radial periodic motion. A frequency is defined by the condition $\nu > 1$ [25]. It is interpreted in terms of GR frequencies ω_r, ω_θ shifted in phase with respect to the classical value of $\omega(cl) = \omega_r(cl) = \omega_\theta(cl)$ so that $\omega_r(gr) < \omega_\theta(gr)$. In this model, the GR effect of the angular precession giving the perihelion advance is defined as the difference $\Delta\omega_(gr) = \omega_r(gr) - \omega_\theta(gr)$. There is no suggestions about possible equations of motion supporting the derivation of the effect, and it is not clear if it is consistent with the traditional value $\Delta\theta_{cen} \approx 43$ arcsec.

The above two approaches to the assessing of the GR perihelion advance use quite opposite assumptions about phase shifts in angular and radial components of orbital motion. In each way, an assumption is made in favor of the desired effect. However, one needs to formulate and validate predictions of Einstein's theory but not its models based on unproved assumptions.

As we know, angular and temporal GR equations of orbital motion have the same (dimensionless) roots. This means that angular and temporal frequency cannot be phase-shifted. The fact that they are shifted in approximate model approaches, tells us that the approximations are in contradiction with the GR Dynamics, so they are flawed.

Our explanation of ambiguity of approximate model approaches goes to the fact that the time dependent GR problem has never been studied, and both the angular solution $r(\theta)$ and the radial one $r(t)$ have never been obtained in the form of the general *exact* solution of the GR equation of motion. We return to this problem in the next subsection, which is devoted to our results of exact full solutions of Einstein's problem and a comparison of the prediction with the Classical theory solutions.

5.4 The notion of time, and the time rate in GR and classical theories

Recall, we use the ideal model of the test particle orbiting about the Sun, mass of which is concentrated in the origin of the fixed coordinate system. The following initial conditions are fixed common for both theories at $t = 0$ and $\tau = 0$, the test particle is positioned at $\theta = 0$; this is a minimal distance

(perihelion) from the Sun r_p with a maximal orbital speed of the particle β_0, while the radial speed is zero $\beta_r = 0$. Next, the denotation of τ_{gr} is used for the time variable in GR Dynamics, and in the classical theory, the time variable is denoted as t_{cl}. Both time variables are dynamic ones measured with the use of standard clocks running uniformly at different rates.

The matter is that Einstein's perihelion advance problem is a special one in GR since it admits local conservation laws in the ideal planetary model, where planets are considered not interacting point-like particles. The planet Mercury is considered the standard test particle probing the field in one-body spherical symmetric problem. The time and angular variables are inalienably connected with the locally conserved angular momentum and total energy. Such a formulation is specific in GR, it admits the Lagrangian approach based on time translation and reverse symmetries yielding the conservation laws, in accordance with Noether's theorem [26]. Consequently, the time τ_{gr} (in GR) and t_{cl} (classical) in each theory is measured by a locally at rest observer, who conducts observations of the test particle (Mercury) in a motion relative to the observer.

As a consequence of conservative properties of gravitational field, it follows that, in physically different GR and classical theories, the standard atomic clocks run uniformly. Not surprisingly, time periods calculated independently in both theories are necessarily different, and suggestion of their equality would be principally wrong. The difference implies that the GR angular perihelion advance must be defined in strict correspondence with the temporal shift. One has to conclude that the time scalings in each theory are linear and proportional to each other with some proportionality coefficient.

5.5 The input data for exact computations of full solutions

For our calculations we used the most recent input data taken from [27, 28, 29], namely:

- the speed of light $c = 299792458$ m/s;
- the Solar mass parameter (heliocentric gravitational constant) $\mu = 1.32712440041 \times 10^{20}$ m^3/s^2, that makes Schwarzschild radius $r_{sch} = 2953.2500770$ m;
- Mercury's perihelion distance $r_p = 4.600 \times 10^{10}$ m;
- Mercury's aphelion distance $r_a = 6.982 \times 10^{10}$ m;

From these data, we have $\rho_0 = 3.21 \times 10^{-8}$. The second parameter $\beta_0^2 = 3.87 \times 10^{-8}$ can be obtained from r_p, r_a and ρ_0. The value β_0^2 has been rounded to three significant figures for fixing identical initial conditions in both classical and GR computations. This makes Mercury's velocity at perihelion $v_p = 5.898 \times 10^4$ m/s, which agrees with [29]. The aphelion value then becomes $r_a = 6.9811764705882 \times 10^{10}$ meters in the classical theory with millimeter precision.

Having the classical initial conditions fixed, the three roots in the GR equation (13) are found exactly, as discussed. The first root, the inverse values of r_p being rescaled $\xi_1 = 1$ corresponds to the perihelion. Now we have the second and the third roots exactly $\xi_2 = 0.65891486$ corresponding to the aphelion, and the third GR term $\xi_3 = 1.5576322 \times 10^7$. Then the GR equation (13) is numerically specified (from here and below, we print up to eight significant digits while the calculations were performed with 600 digits):

$$\left(\frac{\mathrm{d}\xi}{\mathrm{d}\theta}\right)^2 = 6.42 \times 10^{-8}\,\xi^3 - \xi^2 + 1.6589147\,\xi - 0.65891479\,. \tag{39}$$

The corresponding Weierstrass form (27) of the above equation is

$$\left(\frac{\mathrm{d}x}{\mathrm{d}\theta}\right)^2 = 4\,x^3 - 0.083333307\,x - 0.0046296274 \tag{40}$$

with roots $x_1 = -0.083333317$, $x_2 = -0.083333323$, $x_3 = 0.16666664$. However, in SAGE and in PARI/GP we do not need to transform the equation into Weierstrass form in order to compute the periods. The software allows for arbitrary cubic polynomial with scaled major coefficient, produces the corresponding $\wp$ elliptic function and computes the semi-periods. For our input the half periods are $\omega_1 = 3.141592904530036$ and $\omega_2 = 20.40947598338886\,i$. Direct numerical integration reproduces the same result for the orbital half period ω_1 up to 300 significant digits, it is difficult to obtain higher precision for this type of numerical approximation. Taking into account Mercury's sidereal orbit period 0.2408467 Earth years, we obtain the known value of the Mercury's perihelion advance ≈ 42.98 arcsec per century.

It should be noted that such a seemingly small angular advance integral effect in the solution is actually of the order of potential term ρ_0, and it is triggered by the GR cubic differential term $\propto \rho_0\beta_0^2$, which is of the next order smallness in the non-linear equation of motion. This means that it could not

be neglected in any of approximate solutions.

5.6 The criterion of three events

Since the two theories of gravitational field are methodologically different, they have different concepts of time, length, mass etc. To study them in comparison, one needs to normalize physical units. Such a gauging has been actually done in our exact numerical calculations, when the initial conditions were fixed common for both theories, and physical units gauged to fit Earth's physical units in terms of the standard (atomic) clocks. This means that the time unit of one second (the time duration between two sequent ticks) is the same in both theories, and this is also true for other physical units.

Specifically, we compare the results of our study of orbital space and time characteristics focusing the attention on the GR angular and time shifts with respect to the classical theory predictions. The latter reflects Newtonian independent concepts of absolute time and 3-space, while the GR dynamics theory suggests a unique 4-space, in which the time and the 3-space are united by the GR metric.

As emphasized, the GR Mercury's angular advance historically was studied in a separation with the time concept problem. It was suggested that a seemingly tiny difference of time period in GR and classical theories could be neglected in approximate solutions. Contrarily, we solve exactly the pair of GR angular and time dependent dynamics equations and the corresponding pair of classical equations, both pairs being coupled by the constraints imposed by the common initial conditions.

It was found that "the classical atomic clock" runs slower than "the GR clock" that is, the classical time half-period is greater than the GR one by the amount $\Delta t = 0.555$ s (at the starting point, both clocks are set $\tau_{gr} = 0$, $t_{cl} = 0$). Therefore, the GR and classical time lines are related to each other by the following linear expression: $t_{cl} = k\, t_{gr}$ where the coefficient k is a ratio of classical and GR time periods $k = T_{cl}/T_{gr} > 1$. Recall, as the quantitative gauge, the Earth physical units are used.

Our final results are principally different from those obtained by solely computing the GR angular advance of orbital. Still, the question arises, what criterion of comparison should be formulated. Specifically we applied *the three events scheme* formulated in terms of orbital characteristics at three distinct time moments in the GR and classical theories. As a base line, we take the

GR time scale $\tau = \tau_{gr}$ in relationship with similar classical characteristics on the classical time scale t_{cl}.

The three events scheme is suggested in the first half period, as follows:

- Event 1 at the instant τ_1 when $\theta_{gr} = \pi$ (the aphelion is not reached yet).
- Event 2 at the instant τ_2 when the GR aphelion is reached.
- Event 3 at the instant τ_3 when the GR clock displays t_2 value of the classical aphelion (the equality of numbers of ticks of standard clocks in both theories, $\tau_3 = t_2$).

The corresponding time instants t_1, t_2, t_3 displayed by the classical clock follows, as next.

- The instant t_1 corresponds to τ_1 (when $\theta_{gr} = \pi$).
- The instant t_2 is when the classical aphelion is reached.
- The instant t_3 corresponds to τ_3 (when $\tau_3 = t_2$), t_2 is the classical aphelion moment.

5.7 Results of comparison

Let us sum up and discuss the results of three events comparison presented in tables 2 to 5.

In table 2, the common input Mercury's data reflecting the initial conditions are presented. In the output data, the main orbital characteristics are shown for each theory in comparison. Numbers characterizing the differences are rounded up to 4-5 significant digits.

In table 3, the three-events comparison of the GR with respect to the classical theory is shown in numbers: the absolute values of main orbital characteristics at events 1, 2, 3, predicted in each theory, including the time, the radius, the angle, the particle orbital speed, and the passed length. The corresponding absolute and relative differences between the two theories are also given. To the precision of 4 significant digits, differences do not change over the time interval including the three events. From this fact, one can assess the precision requirements to the perihelion observations.

In table 4, the absolute differences of the above variables between events (2, 1), (3, 2), and (3, 1) are shown for each theory.

Finally, in table 5, the projections of each of the three events on GR time scale τ_{gr} to the corresponding classical scale t_{cl} are shown. The main predicted

values of angular shifts and the corresponding time shift are seen in the intervals between events (2, 1), (3, 2), and (3, 1) on each of GR and classical time scales. It follows that the assumption suggesting the equality of time periods in GR and classical theories is not consistent with the comparison criterion based on the combined exact solutions of GR and classical formulation of the Mercury's problem.

It is immediately seen that "the GR particle" compared to "the classical particle", moves on average faster, its aphelion is smaller, consequently, its angular period is advanced by the value 5.019×10^{-7} rad/rev that is, the relative difference of the angle shift with respect to the classical value π is 7.988×10^{-8}; this is the known GR Mercury's perihelion advance. In the time scale, the full time period of the GR orbit is about 1.111 sec/rev shorter than the classical one; that makes a relative difference -1.461×10^{-7}. This temporal effect should be called "the GR temporal advance", which is a replica of the corresponding perihelion angular advance. Their common cause is a tiny non-classical cubic term in (13) of the second order smallness compared to values of the integral GR effects.

The remarkable fact is that the predicted angular advance is accomplished in the time interval between events (2, 1), but the time period difference takes place in the time interval (3, 2). Both angular and temporal effects are nearly doubled if considered in the full interval (3, 1) (from $\theta = \pi$ in GR to the classical aphelion at $\theta = \pi$). In other words, judging by the angular perihelion advance on the GR time line in comparison with half-period time completion, one has to acknowledge that the common GR aphelion does not exists, unless GR Dynamics is exactly reduced to Classical Dynamics by zeroing both effects.

The conclusion has to be made that the naturally looking equality assumption $T_{gr} = T_{cl}$ is principally wrong because it would mean that the GR 4-space curvature structure was replaced with the Newtonian absolute time and space by neglecting the cubic term. Observational tests guided by a chart not accounting for the exact solutions would be misleading.

Let us outline how significant, in our view, are our findings concerning a current status of the GR Mercury's perihelion advance problem.

- There is a belief among physical community including GR researchers that the Mercury's perihelion advance problem formulated by Einstein in November 1915 [1] has been fully studied and understood so that there were no issues to be considered anymore. We state, however, that

it is not true. In this work, it is shown that the problem has never been studied as concerns full (angular and temporal) exact solutions to the GR equations of the test particle motion in spherical symmetric geometry. Only such solutions can reveal a correctly dynamic structure of the GR curved 4-space described by the GR Dynamics.

- The GR prediction of perihelion angular advance apart from a prediction of the corresponding GR temporal shift with respect to the classical picture is not sufficient for understanding the problem at the deeper level and formulating the criteria of a theoretical comparison of GR and classical theories. The small disparity between GR and classical scales of dynamical variables such as time, angle, radius, and others cannot be revealed in the so-called "approximate solutions" and cannot be ignored in the problem of empirical testing of Einstein's theory.
- In a manner of classical theory, the angular and temporal advance increases with a field strength with no restriction. So, it must eventually result in a violation of the Causality Principle in a sense of admitting the superluminal motion. This is confirmed by the exact solutions of the GR strong field phenomena, as seen below. For this and other reasons, we consider below the SR-based approach to the problem, as the alternative to be further studied.
- The presented ideas and findings are novel and constructing, a denial of them would be a discreditation of the real value of General Relativity theory for Astronomy and other applications. We suggest to reconsider the current status of GR particle dynamics together with approximations in methodologies of GR treatments of observations, the required computational and observational precisions, and the criteria of GR verification/falsification. To account for full exact solutions of the problem is the necessity.

6 The GR strong field problem

6.1 Orbital motion

All main equations of GR particle dynamics presented in section 2.2 are valid for the strong field conditions. They are used further in illustrative examples of strong-field problems. In particular, the equation (13), by virtue of the

Schwarzscild metric being an exact solution of Einstein's field model (in the academic GR framework), is claimed to be valid not only under weak field conditions, but also in the whole range of field strength. However, it has never been used for an exact description of the strong fields, particularly, BH environment. Here, for the first time we use the equation for this purpose. Recall, the problem is formulated in the spherical symmetric geometry with the point-like source of mass $M \gg m$, where m is the the point-like mass of the test particle. The central mass can be taken a unit $m = 1$ to be rescaled to physical units when needed.

The abstract point-likeness concept of material bodies is a necessary requirement of the ideal model. In practice, the real size of the source, the radius R is considered in comparison with the gravitational radius r_g or the Schwarzschild radius $r_{sch} = 2\, r_g$, in particular, in "vacuum solutions". For example, for Solar system planets, the radius of Sun $R_\odot \approx 7 \times 10^8$ m is meant when results are physically interpreted. It is not in contradiction with academic study of mathematical properties of the equations. Bearing in mind the ideal model requirements of point-like masses, we found all possible GR exact solutions and their classification, including those for strong fields (previously discussed).

In literature, the GR particle orbital motion in strong gravitational fields is often associated with the Black Hole environment. The concept of Black Hole used in Astrophysics suggests that a material spherical object having several solar masses, undergoes the hypothetical process of gravitational collapse. This is a hypothetical phenomenon rather than a mathematical abstraction. It does not follow from the GR academic framework we use. Moreover, it is completely estranged from the Standard Particle Model.

The GR equation of motion implies the conservation laws and periodic time-reversal solutions, so that the test particle never perish in a collision with an ideal point like center. Lagrangian properties are always preserved, particularly, in spiral fall orbits. As the parameter $\beta_0^2 \to 0$, the orbital precession frequency and the particle speed rapidly increase.

An example of orbital motion in a moderately strong field is shown in fig. 7 with the following parameters: $\rho_0 = 0.05$, and $\beta_0^2 = 0.04$. As seen from orbit classification table 1, it is of sub-circle type with notably precessing orbit. The angular half period there is about 4.53 radians, which is by 44% larger than the corresponding classical value π, the time period is by 7% smaller,

the periapsis by 38% smaller, and the velocity at periapsis by 63% higher.

6.2 Spiral fall and the particle speed

The spiral fall orbit does not have an analogy in the classical theory. This is the GR phenomenon in the strong field in the sub-circle orbits, when the roots ξ_2 and ξ_3 approach each other. The case $\xi_2 = \xi_3$ is "the edge point" so that the spiral fall occurs in the region where the roots ξ_2 and ξ_3 become complex numbers, fig. 9. More details about spiral fall formation can be found in [4]. The particle can start from the initial weak field condition and fall upon the center under extremely strong fields before returning back with a huge angular advance. For $\rho_0 > 1/4$, the only possible type of Black Hole orbits is of spiral fall, as seen from tables and figures of orbit classification. An example of typical spiral fall orbit is shown in fig. 5.

The angular advance and total speed of the test particle increase with $\sigma = \rho_0/\beta_0^2$. There is no mechanism in GR Dynamics, which can restrict this tendency, hence, it is possible that the particle would move faster than light. This issue is discussed in the textbook [25] in connection with a radial fall (the exact full solution of the orbital motion problem was not available at the time when it was published). They correctly concluded that the superluminal motion can occur after the particle crossed the Schwarzschild surface of radius $r_{sch} = 2\, r_g$.

The existence of superluminal motion is confirmed as one of results of our exact solutions of orbital motion. From the conservation laws in the case of non-zero angular momentum, we obtain the expression for the total speed of the particle along an orbit:

$$\beta^2(\xi) = \beta_0^2 - 2\,\rho_0 - 2\,\rho_0\,\beta_0^2 + 2\,\rho_0\,\xi + 2\,\rho_0\,\beta_0^2\,\xi^3\,. \tag{41}$$

From this, the total speed at Schwarzschild radius is found in terms of elementary functions

$$\begin{aligned} v^2(r_{sch}) &= 1 - 2\,\rho_0 + \beta_0^2\left(1 - 2\,\rho_0 + \frac{1}{4\,\rho_0^2}\right) \\ &= (1 - 2\,\rho_0)\left(1 + \beta_0^2\right) + \frac{\beta_0^2}{4\,\rho_0^2}\,, \end{aligned} \tag{42}$$

with radial and angular velocities given by eqs. (9) and (10).

Depending on the initial velocity, the full speed at Schwarzschild radius can be smaller than, equals to or greater than the speed of light. Fig. 13 shows the condition on ρ_0 and β_0^2 in order to achieve the speed of light at Schwarzschild radius. Example of a spiral fall trajectory from case 3 of fig. 9 is shown in fig. 10. The particle crosses the Schwarzschild surface at the speed $\beta_{sch} = 1.982$ and continues to accelerate.

Let us consider the components of velocity for particle crossing the horizon $\xi_{sch} = 1/(2\,r_g) = 1/(2\,\rho_0)$, also in exterior and interior regions. On the horizon sphere, the GR effective potential always takes a zero value, $V_{eff}^2 = 0$ (straightforward verification). Consequently, the squared radial speed is equal to the total (squared) energy, $\beta_r^2 = \epsilon_0^2$ always taking values less than unit, $\beta_{sch}^2 = \epsilon_0^3 < 1$ in the whole range of interior region (including the Schwarzschild surface).

The orbital component could be any, depending on β_0^2. Indeed, $l_0 = r_0\,\beta_0 = r\,\beta_\theta$, $r = 1/\xi$ or

$$\beta_\theta(\xi) = \beta_0\,\xi\,, \quad \beta_\theta^2(\xi) = \beta_0^2\,\xi^2\,. \tag{43}$$

At a however small β_0^2, a however small (squared) addition to the radial speed makes the resultant speed less than the speed of light, $\beta < 1$, or, at some greater value, makes $\beta \geq 1$, as in the example of fig. 10.

One would like to know from our results how fast a particle moves in a spiral fall in the exterior and interior regions that is, before and after crossing the Schwarzschild surface, the so-called horizon. This question never arose in literature because of common belief that a particle in spiral fall always crosses the horizon at the speed of light. However, such a belief does not have a rigorous proof, it rather comes from arguments based on suggested formulas with no association with the equation (1).

Figures 11 and 12 demonstrate GR predictions of particle motion in the interior (and while crossing the horizon) with speed less and greater than the speed of light. In the example of field strength $\rho_0 = 0.050$, we have the following speed (squared) values at the horizon $\xi_{sch} = 10$:

- subluminal case, $\beta_0^2 = 0.0001$, Figure 12: $\beta^2 = 0.910$, $\beta_r^2 = 0.900$, $\beta_\theta^2 = 0.010$;
- superluminal case, $\beta_0^2 = 0.0080$, Figure 11: $\beta^2 = 1.707$, $\beta_r^2 = 0.907$, $\beta_\theta^2 = 0.080$.

- For a greater value of $\beta_0^2 = 0.030$ (still less than the edge value $\beta_0^2 = 0.03419$), it would be $\beta^2 = 3.927$, $\beta_r^2 = 0.927$, $\beta_\theta^2 = 0.300$.
- It is easy to find that the particle crosses the horizon at the speed of light for $\rho_0 = 0.005$, $\beta_0^2 = 0.0010$: $\beta^2 = 1.000$, $\beta_r^2 = 0.900$, $\beta_\theta^2 = 0.100$.

6.3 Free radial fall

As previously noted, GR Dynamic equations of orbital motion are reduced to classical ones when the GR cubic term of interference of angular momentum with the potential energy is neglected. Because the angular momentum of the particle in free radial fall is zero by definition, the GR equation of the radial motion has to be automatically coincide with the corresponding classical one, provided the appropriate initial conditions are fixed.

In conventional GR Dynamics, however, the radial fall equation differs from the classical one. The reason for that is that the GR equation is derived with the use of GR expression of conserved total energy ϵ_{rad} (7) [30], also [25, 31]. Recall, unlike in orbital motions, in the GR case of a radial fall, we have two time variable, τ and t, having different meaning.

Below, we follow the conventional derivation of equations starting from the initial conditions in the expression for ϵ_{rad}:

$$\epsilon_{rad} = (1 - 2\,r_g/r)\,\mathrm{d}t/\mathrm{d}\tau = (1 - 2\,r_g/r_{ic})\,\mathrm{d}t_{ic}/\mathrm{d}\tau_{ic}\,. \tag{44}$$

Assume the initial conditions are fixed at "far away". To avoid the infinite time of motion from infinity, let us introduce the "far-away" distance r_{fa} however great but finite, and let the initial inward speed be $(\mathrm{d}r/\mathrm{d}t)_{fa} = (1 - 1/\gamma_{fa}^2)^{-1/2}$. Then, the inward speed of a particle in the radial fall is found:

$$(\mathrm{d}r/\mathrm{d}t)_{fa}(r) = (1 - 2r_g/r)\left(1 - (1 - 2r_g/r)/\gamma_{fa}^2)\right)^{1/2}\,. \tag{45}$$

Here, $\gamma_{fa} = E_0/m_0 \geq 1$ is considered the "far-away" total energy. Respectively, the formula is interpreted in terms of the "far-away" observer whose wristwatch shows the coordinate time t. At the same time, let us introduce the so-called "shell observer" placed at some point $r_{shell} < r_{fa}$, which is not fixed in the initial conditions, whose wristwatch must show the proper time τ_{shell}. Then, the radial speed $\mathrm{d}r_{shell}/\mathrm{d}\tau_{shell}$, viewed by the "shell" observer in

accordance with (44), must be given by

$$(\mathrm{d}r/\mathrm{d}\tau)_{shell}(r) = \left(1 - (1 - 2r_g/r)/\gamma_{fa}^2)\right)^{1/2} . \tag{46}$$

The formula (45) has to be understood from the viewpoint of "far-away" observer. It shows that the particle sent from infinity to the center begins to accelerate, but at some point, it starts decelerating. The motion looks "strange", however. The matter is that the particle, before approaching the Schwarzschild radius $r_{sch} = 2r_g$, at some point dependent on γ_{fa}, starts decelerating: the higher initial kinetic energy, the farther the deceleration point from the center. For $\gamma_{fa} \geq \sqrt{3/2}$, the particle will never accelerate in a gravitational field. The gravitational force exerted on the particle becomes repulsive in the entire space.

Quite differently, the formula (46) shows that, from the viewpoint of "shell" observer, the particle always accelerates. When crossing the Schwarzschild sphere, it reaches the speed of light. In the internal space, the particle is considered not observable (due to "light trap"), likely, its motion becomes superluminal till it "crashes" at the center. This picture is widely known in association with the particle radial fall onto Black Hall.

We consider the radial motion the ideal case of a pure academic interest because the requirement of the exact zero angular momentum is physically not realistic.

7 The Special Relativity theory

7.1 Transition from the abstract proper 4-space to the observable coordinate space-time

In this work, we challenge the statement that, unlike Einstein's General Relativity theory, the Special Relativity theory is not able to describe the Newtonian gravity [30]. They say that SR Dynamics failed to explain observations of Mercury's perihelion advance in the gravitational field of the Sun, and some other observations. The objection points to the fact that the argument of incompatibility with gravitation is based on certain assertions and actually not strictly proven [32]. In particular, it is shown that an introduction of the relativistic concept of field dependent proper mass makes the difference.

SR Dynamics (motion in field of forces) starts from the concept of the abstract proper 4-space x^μ known in connection with the earlier developed SR Kinematics (motion by inertia with no forces). In both cases, the proper 4-space is converted to the coordinate space-time, in which SR Kinematics and Dynamics is formulated in the real physical space and time.

The starting point is the concept of a world line $s(x^\mu)$ characterized by the abstract proper time τ serving the role of affine parametrization of space and time variables (with a usual convention of speed of light at infinity $c_0 = 1$). The metric quadratic form in the *abstract* 4-space is given by

$$\mathrm{d}s^2(\tau) = c_0^2\,\mathrm{d}\tau^2\,. \tag{47}$$

The proper unit 4-vector $U^\mu = \mathrm{d}(x^\mu)/\mathrm{d}s$ is introduced, which is tangential to the world line, so that the metric tensor is diagonal:

$$U_\mu U^\mu = 1, \quad U_\mu(\mathrm{d}U^\mu/\mathrm{d}\tau) = 0\,. \tag{48}$$

The proper 4-coordinate infinitesimal displacement $\mathrm{d}x^\mu$ of the world line is defined in connection with the 4-space and the 4-momentum (complementary) space P^μ through U^μ:

$$\mathrm{d}x^\mu = \mathrm{d}\tau(x^\mu)U^\mu, \quad P^\mu = m(x^\mu)U^\mu\,. \tag{49}$$

Next, the 4-vector force in the abstract proper 4-space is defined

$$K^\mu = \mathrm{d}P^\mu(s)/\mathrm{d}s\,. \tag{50}$$

This is the Minkowski 4-force having, as any 4-vector, the proper (temporal) part and spatial components of 3-vector. One can proceed further in a formulation of the angular momentum, the torque, etc. in the tensor form similarly to that in Relativistic Electrodynamics.

Eventually, all abstract physical quantities are put in connections with real measurable or observable quantities in physical world. For example, the Minkowski 4-force is associated with the scalar, – the conserved total energy, and the components of "ordinary" force, – the vector in 3-space [33].

The Lorentz transformations is the main tool of conversion of the abstract 4-space to the coordinate space-time, what is *the observable* Minkowski space-time. Similarly, the abstract 4-momentum is connected with the correspond-

ing real physical quantities. At the same time, the SR Lagrangian formulation of the problem is important in the generalization of SR Kinematics to the SR Dynamics.

With the transition to the coordinate (the observable) space-time, one can forget the abstract proper 4-space and the abstract equations there. Unfortunately, a terminology of "proper quantities" is used for observables also, – in a sense of the observables at rest with respect to imaginary observers exchanging their information with respect to each other in a relative motion. In the operational language, they do it using the standard (atomic) clocks serving also the role of the standard emitter/detector of the light signal.

7.2 Field dependent proper mass

In the conventional SR theory, the proper mass is constant. We consider it a weak field approximation, after Synge, [33], who developed the theory accounting for the proper mass variation in the field but thought the effect be practically negligible, as a reasonable approximation. This point of view is widely accepted among the Relativistic Mechanics community. The history of this issue and the consequences of the approximation are discussed in [32], also see [34].

The advanced SR particle dynamics is formulated in the coordinate space-time of observables, where the static mass or the mass in the comoving reference frame (both usually called the proper mass, as noted) are field dependent proper mass. In the static spherical symmetric field, a dependence of the proper mass on radius is given by

$$m(r) = m_{test} \exp(-\rho_0(r_0/r)) \,. \tag{51}$$

Here, m_{test} is the mass of the test particle having a limit $m(r) = m_{inf}$ as $r \to \infty$. As shown below, it can be considered in relations with the Einstein-DeBroglie's concept of the standard clock characterized by the frequency of ticks, what allows the comparing the time rate as the field strength (the potential function) changes. In the ideal (one body) model, the test particle mass is canceled on left and right sides of the SR equations of motion, similarly to that in Classical Dynamics.

Thus, the static potential function in the space-time coordinate space takes

the form

$$V(r) = -\left(1 - \exp(-r_g/r)\right) , \tag{52}$$

which is reduced to Newtonian potential $V(r) \propto 1/r$ at $r_g/r_0 \ll 1$.

To consider the proper mass constancy "an approximation" would be actually methodologically wrong because the values of $\mathrm{d}t$ and m must be inversely proportional due to the complementarity of the SR space-time vector and $\mathrm{d}x^\mu$ and the 4-momentum vector P^μ, therefore, their scalar product is constant:

$$P^\mu \cdot \Delta x_\mu = m\Delta t\,. \tag{53}$$

It is the absolute value of constant 4-phase vector. It is consistent with the Einstein-de Broglie relationship. There, a period of a quantum oscillation is related to the frequency

$$mc_0^2 = h\,f, \quad \Delta\tau = 1/f\,, \tag{54}$$

where h is Planck's constant, $c_0 = 1$, $m_0 = 1$. Next, we take $\mathrm{d}t = \Delta t$ meaning a however small finite period of the standard quantum oscillator in (54) (the time interval between consequent clock's ticks).

We have to reiterate that SR Dynamics with the field dependent proper mass is fully relevant to the relativistic motion in the gravitational field, and it obeys the Causality Principle (as follows from the SR Dynamics formulation and the corresponding equations). Also, we make a strong statement that the known central infinities in the existing field theories would be naturally eliminated with the introduction of the field dependent proper mass in the spherical symmetric geometry. Consequently, the force on the test particle has a zero limit as the radius approaches the center. This fact is illustrated in fig. 14.

Remarkably, the picture reminds the QCD phenomenon of "quark rad/rad overrad/rad overconfinement" related to "the asymptotic freedom". The artificial mathematical procedures of "mass renormalization" became not needed. For this and other reasons, we suggest SR Dynamics be considered the alternative to GR particle dynamics [3, 32, 35].

Next, the principles of advanced SR Dynamics applied to the spherical symmetric field, and the corresponding orbital motion equations are formulated.

7.3 Principles and equations of SR Dynamics

In brief, the SR Dynamics problem of orbits is formulated in the relativistic Lagrangian approach consistently with Noether symmetries of space-time (the 3-space isotropy, and the coordinate time translation and time reversal) in relationship with the conservation laws. Therefore, the coordinate time t runs uniformly while the comoving observer's time pace t_{com} is affected by the field.

In polar coordinates, the 4-coordinate displacement vector and the 4-momentum vector are defined, as follows: $\mathrm{d}X^{\mu}(r) = \gamma\,\Delta t\ (1, \beta_r, \beta_\theta)$ with the Lorentz factor $\gamma = (1-\beta^2)^{-1/2}$, β is the total orbital speed. The 4-momentum vector is $P^{\mu}(r) = \gamma\, m(r)\ (1, \beta_r, \beta_\theta)$, where 3-velocity components and the Lorentz factor are functions of r and θ, with a usual convention $c_0 = 1$.

We shall see that the equations of motions are characterized by two roots. In other words, the equation of motion in a dimensionless form is governed by two independent physical parameter. In this sense, there is a similarity of the GR and SR Dynamics but the results would be radically different because the principles of SR Dynamics do not allow superluminal motion in any circumstances.

In terms of initial conditions, there are only two independent physical parameters, which are parameters of the equations of motion, for example, the field strength ρ_0 and the squared angular speed β_0^2, their ratio being the classical orbit classification parameter $\sigma_0 = \rho_0/\beta_0^2$. Also, we may use the analogous relativistic parameter $\sigma_r = \gamma^2\sigma_0$.

There are two conservation laws, – the conserved total energy ϵ_0, and the conserved angular momentum L_0 given below for the initial conditions $r(r) = r_0$, $\theta = 0$, $\beta_r = 0$, $\beta_\theta = \beta_0$:

$$\epsilon_0 = \gamma_0\,\gamma_{r,0} = \gamma\,\gamma_r\,, \tag{55}$$

$$L_0 = \gamma_0\,\gamma_{r,0}\,r_0\,\beta_0 = \gamma\,\gamma_r\,r\,\beta_\theta\,. \tag{56}$$

Instead of (56), it is convenient to use a conserved quantity $l_0 = \epsilon_0/L_0$:

$$l_0 = r\,\beta_\theta\,. \tag{57}$$

Here, a squared inverted Lorentz factor is $1/\gamma^2 = 1-\beta_r^2-\beta_\theta^2$, and $\beta_r = \mathrm{d}r/\mathrm{d}t$, $\beta_\theta = r\,\mathrm{d}\theta/\mathrm{d}t$. To get the angular equation, consider $\beta_r = (\mathrm{d}r/\mathrm{d}\theta)(\mathrm{d}\theta/\mathrm{d}t)$, and transform (57) into $\beta_\theta^2 = l_0^2/r^2$. After introducing a variable $\xi = r_0/r$, we

arrive to the exact relativistic equation of orbital motion of a bounded test particle. The equation is valid for a however strong field by the criterion r_g/r:

$$\left(\frac{\mathrm{d}\xi}{\mathrm{d}\theta}\right)^2 = \frac{1}{\beta_0^2} - \xi^2 - \frac{1}{\gamma_0^2\,\beta_0^2}\,\exp\left(\frac{2\,r_g}{r_0}\,(1-\xi)\right)\,. \tag{58}$$

The Newtonian limit, or weak field conditions, is given by a linear approximation of the exponential function:

$$(\mathrm{d}\xi/\mathrm{d}\theta)^2 = (1-2\,\sigma_r) + 2\,\sigma_r\,\xi - \xi^2 - 2\,\sigma_r\,(r_g/r_0)\,(1-\xi)^2\,, \tag{59}$$

By definition, there is a useful relationship

$$\mathrm{d}\xi/\mathrm{d}\theta = (\mathrm{d}r/\mathrm{d}t)/\beta_0\,, \tag{60}$$

where $(\mathrm{d}r/\mathrm{d}t)^2 = \beta_r^2(r)$ is the radial (squared) component to the total (squared) speed $\beta(r)$:

$$\beta^2(r) = \beta_r^2(r) + \beta_\theta^2\,, \tag{61}$$

with the angular speed term

$$\beta_\theta^2 = r_0^2\,\beta_0^2/r^2\,. \tag{62}$$

The particle speed at free radial fall is:

$$\beta(r) = \left(1 - (1/\gamma_0^2)\,\exp(-2\,r_g/r)\right)^{1/2}\,. \tag{63}$$

8 The Mercury problem in SR Dynamics

In a full analogy with quantitative comparison of GR Dynamics with respect to Classical Dynamics of orbital motion, we introduce the three event scheme comparison of SR Dynamics with respect to Classical Dynamics. Unlike in GR, the SR events delay with respect to classical time instants. The three event instants on the base SR time line t_{sr} are defined, as follows.

- Event 1 at the instant $t_{sr,1}$, when SR clock displays the value of the classical aphelion, the event 2 (the equality of numbers of ticks of standard clocks in both theories, $t_{sr,1} = t_{cl,2}$).
- Event 2 at the instant $t_{sr,2}$, when the SR aphelion is reached.

- Event 3 at the instant $t_{sr,3}$, when the SR orbital angle is π.

The corresponding time instants t_1, t_2, t_3 displayed by the classical clock are specified, as well:

- The instant t_1 corresponds to $t_{sr,1}$ (when $t_{sr,1} = t_{cl,2}$).
- The instant t_2 is when the classical aphelion is reached.
- The instant t_3 corresponds to $t_{sr,3}$ (when the SR orbital angle is π).

Results of comparison based on the 3 events scheme for the exact combined solutions of the Mercury problem in SR and Classical Dynamics are presented in tables 6 to 9.

In table 6, the input and output data for computing Mercury's orbital characteristics in Classical and SR Dynamics are given. In the input, must be only two independent model parameters, for example, ρ_0 and β_0^2. In the output, absolute values of main classical characteristics integrated over the full period and their absolute and relative differences with respect to corresponding SR Dynamics results are given.

In table 7, orbital characteristics q_{sr} computed at 3 events in SR Dynamics time scale t_{sr} in comparison with q_{cl} computed in the classical time scale t_{cl} starting with initial conditions. Also shown their absolute and relative differences $\Delta q = q_{sr} - q_{cl}$, $\delta q = (q_{sr} - q_{cl})/q_{cl}$. The following characteristics are computed: the time passed t_{sr}, t_{cl}, the radius r_{sr}, r_{cl}, the orbital angle r_θ, r_θ, the orbital speed v_{sr}, v_{cl}, the orbital length l_{sr}, l_{cl}.

In table 8, absolute differences of orbital characteristics between events (2, 1), (3, 2), (3, 1) computed in SR Dynamics and Classical theory.

Finally, in table 9, the projection of the three SR events on the base time line t_{sr} and the classical time line t_{cl} is shown. Notice, dealing with disparity of events on time and angular scales, one has distinguish between the angle π in Classical and and Relativistic theories.

Similarly to the GR Mercury problem, the corresponding SR time instants t_1, t_2, t_3 displayed on the time lines are specified, where the standard clocks run uniformly in both theories too. However, the standard "SR clock" on the base time line runs slower than "the classical clock". The SR and classical time lines are related to each other by the following linear expression: $t_{cl} = k\, t_{sr}$ where the new coefficient k is a ratio of classical and SR time periods $k = T_{cl}/T_{sr} < 1$. Again, it is a disparity of SR and classical time lines, which requires a necessity of difference in SR and classical time periods.

The relativistic SR effects characterize the retardation of the angular and temporal rates with respect to the classical theory predictions. Namely, in a first half period, starting from the initial conditions, the angular shift $\Delta\theta = -8.365 \times 10^{-8}$ rad, or the relative effect $\delta\theta = -2.663 \times 10^{-8}$, are delayed with respect to the classical theory. The effect is three times smaller but has an opposite sign than the corresponding GR effect. The about same factor of retardation is seen in the time half period where the difference is $\Delta t = 0.191613$ s, or the relative effect $\delta t = 5.042 \times 10^{-8}$.

Clearly, the SR retardation is due to the proper mass dependence on the field strength implemented into SR Dynamics. It must prevent the particle motion from the appearance of superluminosity under strong field conditions: with the rise of a field strength, the particle motion rise is restricted by SR laws. Moreover, the central infinity is naturally eliminated and more positive consequences follow, and the Black Hole GR concept and other String field phenomena are revised.

The retardation of SR angle is equivalent to the angular classical advance, so we suggest the following law of the angular shift under weak field conditions analogous to the GR angular advance, (33). Its precision increases with the decrease of field strength

$$\Delta\theta = \sigma_0\,\rho_0 \tag{64}$$

Here, $\Delta\theta = \theta_{cl}/\theta_{sr} - 1 = \sigma_0\,\rho_0$ is a relative angular advance rad/rad of the classical angle with respect to the SR angle (initially averaged over half a period), $\theta_{cl} = \pi$, $\sigma_0 = \rho_0/\beta_0^2$ for $\rho_0 \ll 1$. As opposed to GR, the value of the angular shift in SR Dynamics with respect to the Classical theory is exactly 3 times less than in GR, but has an opposite sign. The time period is greater in SR Dynamics by about the same factor 3 of retardation.

As noted earlier, the observational tests are out of scope of this theoretical work. One can argue nevertheless, that observations are consistent with the GR angular advance anyway, so why do we need to consider the alternatively predicted "retardation" anyway?

Our counter arguments follows from the statement that, in view of the exact GR temporal solution, the GR confirmation criterion needs to be re-considered, in particular, due to our finding that the GR prediction of about one second difference of classical and GR periods $\Delta T = T_{cl} - T_{gr}$ needs to be observationally "confirmed" too. This requires a stabilization of observational tools to the precision, at least, 0.1 sec over one or more periods (this

looks hardly possible today for many practical reasons, but this matter must be actually judged by professional Astronomers). From the SR Dynamics predictions, even higher precision of space-time observations is required.

We conclude that, in the alternative to GR Dynamics, – the SR based Dynamics, the GR controversies and problems, related, in particular, the superluminosity in a sense of Causality Principle breakage, infinities, τ vs t time variables, and others, do not arise.

9 Comments on additional topics: Gravitational Waves, and GPS

The physical phenomenon of Gravitational waves (GW) is allegedly one of the GR predictions. According to the nowadays views, allegedly detectable GWs originate in very strong fields during spiral merges of supermassive Black Holes (BHs). Einstein's field equations (EFEs) along with GR Dynamics are supposed to provide a reliable theory, which rigorously, fully, and consistently explains the GW phenomenon in the whole range of field strength. From our study, however, it follows that GR explanations, which are made in terms of "metric waves", encounter numerous fundamental contradictions with the GR basic concepts.

The Global Positioning Systems (GPS) is practically used in weak fields of planetary system, first of all, under the Earth conditions. The GPS requires an extremely high precision of functioning and fast operational control of the database. Its theory is based on theoretical approximations claimed to be GR weak field approximate GPS model. Strangely enough, there were no attempts to exactly solve the Relativistic Dynamic equations in the GR framework and compare the results with the classical theory. From our study, it follows that the existing theoretical GPS model is in conflict with the GR Dynamics.

There is numerous historical and modern literature devoted to each (GW and GPS) of the problems. The reason of our brief comments on them is a continuing arguing about whether the GR theory is satisfactory for physical explanations and quantitative predictions of the corresponding observations and predictions. The Author's critical view on the GR problems presented below is arguable and intended to stimulate among Physical Community new discussions beyond main-stream theories.

9.1 The GR phenomenon of gravitational waves

The GR basic theoretical concepts in GW theory

Among GR, Astrophysical and Cosmological communities, new detection opportunities of the GW due to a progress of technology is considered the fundamentally important step for unveiling not answered yet quests about physical world we live in, see "The Gravitational Wave International Committee Roadmap", [36, 37], GW calculations [38, 39], the future of gravitational wave astronomy, [40]. The history of the problem is given in [41], the current status and perspectives see in [42], see also detailed presentation of the GW problem [30]. There are numerous specific aspects of observations, explanations, and predictions appear in the growing literature.

Here, facts concerning the GR mathematical theory of GWs are outlined.

On GR inconsistency with Fundamentals of Physics

The GR as "geometrical gravitation" is inconsistent with Modern Physics branches such as SR Kinematics and Dynamics, Quantum theory, Particle Physics. The GR, supposed to be a theory beyond Newton's gravitational force *instant* action at distance, but contrary, it ignores the fundamental concept of relativistic field of forces acting at distance. Instead, it suggests local metric "disturbances" and their propagation with the speed of light (GWs) in the proper coordinate system so that the speed depends on the choice of coordinate system. Consequently, the GR violates the Causality Principle in terms of particle motions slower than light. The GW concept is claimed to be developed in the GR framework in the whole range of field strength. In practice, it is based on metric linearization, – the PPN (weak field) approximation, which is actually not sufficient for the purpose. There is a common belief that the GR is reduced to the Newtonian limit for a body in slow motion in weak fields. However, this belief is not true, as shown in this work. It is clear that the GR major flaws are rooted in Einstein's field equations (EFEs).

EFEs

The equations are formulated for Lorentzian manifolds defined by the proper 4-space metric $\widetilde{\mathrm{d}s} = c_0\mathrm{d}\tau$. All admitted solutions have the time variable τ while observations are conducted in the coordinate space-time with the time

variable t. This causes fundamental problem of solution interpretation when the GR predictions are compared with observations.

There are only two physically meaningful types of solutions admitted by EFEs:

a) The vacuum one-body solutions with the point source of mass M. Typically, it is the Schwarzschild field and the corresponding geodesics for a point test particle of mass $m \ll M$.

b) The metric space expansion in Cosmology for a continuous matter distribution. The N-body problem ($N > 1$) has no GR solution. Here, we are restricted to the $N = 1$ (one-body) vacuum solution, which is not reducible to the Newtonian limit for typically 2-body problems.

In GR, there are no local conservation laws. However, in the vacuum solution (the one-body problem), the force acting on the test particle is conservative because of $m \ll M$. There is a price for it: the force keeping the test particle in orbital motion is not gravitational; it is a non-inertial or "tidal" force, which is due to the space-time curvature.

Actually, in all types of GR problems, the gravitational field is interpreted in terms of non-inertial or tidal forces. Genuine gravitational field would appear in a pseudo-tensor form, and for this reason cannot be added to the matter part in the stress tensor when geodesics are derived. The gravitational world constant G is introduced there not from the GR first principles but solely for making normalized solutions similar to those in Newtonian gravity.

The above listed GR drawbacks prevent the formulation of GW problem for practical use. There are other reasons, discussed in publications, for doubting the GW detection by LIGO.

LIGO today

As of today, the working GW model seems hardly different from that in [30]. As before, it is affected by the GR concept of gravitational field, which is the field of non-inertial and tidal forces. It excludes the genuine gravitational force and corresponding scalar potential field, studied by Newton and his counterparts. This embarrassing property is not discussed by GR experts.

In comparing the electromagnetic waves (e/m), which follows from relativistic electrodynamics, one can see there Fundamental Physical Principles governing the e/m radiation. This is, firstly, the Causality Principle ensured

by inductive properties of "empty" space, namely, its characterization by the electric permittivity ϵ and the magnetic permeability μ. They are in intimate relationship with the value of speed of light c. As a transverse wave, light is naturally driven by consequent changes of electric and magnetic components (the induction process). The same processes take place in transmitting and detecting antennas. The second Fundamental Physical Principle is valid for isolated systems. It manifests the conservative properties of e/m forces in relationship with space-time symmetries. It follows that the e/m waves can originate only at the expense of energy from an external energy storage. Those Principles fully explain the nature of e/m origination, emission, propagation, and detection, however, they are completely broken in the GR Foundations. The GW is not a physical wave but rather a metric wave that is, a motion of a specific metrical disturbance among numerous other disturbances depending on the choice of a coordinate system. The physical cause of the existence of such type of GW is not clear. The claimed cause is all types of acceleration of massive body, likely, in analogy with the e/m radiation from accelerated charged bodies. But this analogy is wrong. The most important doubt concerns a replacement of Newtonian gravity (allegedly reduced from GR in PPN approximation) by a field of non-inertial and tidal forces (which are actually results of e/m forces).

There are a lot of contradictions of GR concept of GW, as seen from our studies of exact solutions. For example, geodesics of test particles and GWs are derived in terms of temporal variable τ, which is replaced by the coordinate time t with no comments. Typical GW sources are pairs of merging BHs, which is the two body problem not admitted by EFE solutions. The system of two bounded bodies are subjected to conservative fores, which cannot generate GWs. The BH in GR is not observable. A typical merging process of two BHs takes a huge time by Earth's clock, not a short "flash" time. It is also not clear, how, in several detection events, the GW source were specified in so many details.

A typical objection to the GW *metric* waves is the statement: if the photon wavelength stretches as the LIGO antenna does, the gauge change and the interferometric phase shift would be unobservable. To make them observable, the perturbed gauge should be compared with the original one (before perturbation) at the time of GW detection, but this is not the LIGO case. The GR expertise answer to the objection is related to a role of the GW quadrupole

model. This is not a satisfactory explanation because an interferometric phase shift is no way restricted by the wave configuration.

The conclusion is that the LIGO concept is based on assumptions, which are not substantiated, GW Physics is not clear and contradictory. The attention needs to be focused on the LIGO fantastic sensitivity to a tiny spatial shift being about 3 orders smaller than the proton size. The accuracy of stabilization of LIGO functioning at this regime (an uncharted QM region) is not clear for us.

9.2 The GPS problem

Below, our comments concern a development of GPS theoretical model based on the GR methodology of space-time curvature caused by massive bodies. This methodology somehow differs from that of GW, but its GR principles remain the same.

The GR-based Model of GPS

A history of GW and GPS problems are dated back to early nineteenth, when contemporary GR ideologists laid out GPS basic ideas. In [43], it is emphasized that a successful realization of the GPS Project is vitally important for future new technologies, but it would depend on clear understanding of the radically new GR theory based on the space-time being curved by massive bodies. A sketch of "a conceptual GPS Model" is drawn there. Unfortunately, it is far beyond capacities of the Author of this work to catch it.

In a reputed work [25], the problem academic formulation for scientific communities begins with the Schwartzschild metric (earlier discussed in this work). In our view, it demonstrates an approach, which is, in some parts, inconsistent with GR or even physically erroneous. Luckily, the practical development and realization of GPS project in 1995 by special teams of engineers and experts were carried out independently of academic works [44]. There, the gravitational time dilation and SR motion dilation are taken into account, what is a reflection of numerous works on GPS [45].

From [25], we have

$$\mathrm{d}\tau^2 = (1 - 2\,r_g/r)\,\mathrm{d}t^2 - (1 - 2\,r_g/r)^{-1}\,\mathrm{d}r^2 - r^2\,\mathrm{d}\theta^2\,, \tag{65}$$

where $c = 0$, hence, time variables are measured in length units. Let apply

the equation twice: firstly, to the GPS clock orbiting with the constant speed, $\mathrm{d}r = 0$ (for example, in the equatorial plane), secondly, to the clock located on the Earth (the equator), both uniformly rotating around the Earth's center. From it, let us make

$$(\mathrm{d}\tau/\mathrm{d}t)^2 = 1 - 2\,r_g/r - r^2\,(\mathrm{d}\theta/dt)^2\,, \tag{66}$$

where $\mathrm{d}\tau$ is the wristwatch time interval between ticks of either atomic clock, and $r\,\mathrm{d}\theta/\mathrm{d}t = v$ – a circular speed measured by "the bookkeeper" far away. Consequently,

$$(\mathrm{d}\tau/\mathrm{d}t)^2 = 1 - 2\,r_g/r - r^2\,(\mathrm{d}\theta/\mathrm{d}t)^2\,. \tag{67}$$

There, $\mathrm{d}\tau = \mathrm{d}t_{gps}$ either $\mathrm{d}\tau = \mathrm{d}t_{earth}$. From the above, it is suggested to make the equation to be linearized for further work:

$$\left(\frac{\mathrm{d}t_{gps}}{\mathrm{d}t_{earth}}\right) = (1 - r_g/r_{gps} - v_{gps}^2)^{1/2})(1 - r_g/r_{earth} - v_{earth})^{-1/2}\,. \tag{68}$$

Next, the authors suggest readers to practice and confirm that the GPS clock runs faster by about 50 000 nanoseconds, but it is not clear from this what relativistic effects are. Neither it's clear why one needs to put the Earth rotation and the GPS orbital rotation on the same footing. A speed v_{gps} and the orbital time T_{gps} are determined by the GPS geodesics in classical and GR theories, and a small difference between GR and classical dynamics results must be found. However, the authors construct the whole GPS Model using static parameters instead of formulating equations of motion and solving them. As for Earth rotation, it is not relevant to the above equations, it is rather a separate issue of choosing the right coordinate systems, in which the GR technical triangulation problem is to be solved.

It is not clear at all, why the GPS problem is not considered here in an analogy with Mercury problem. As discussed in this work, the latter has been thoroughly studied in GR with the result of the GR perihelion advance $\Delta\theta = 3\sigma_0(r_g/r_0)$ in dimensionless form. From this result, it is easy to assess the corresponding GPS temporal advance of the circular orbit. Such an effect a relativistic effect there is quite significant in the GPS motion and could be tested provided theoretical experts focused GPS researchers' attention on this approach and clearly formulated the predicted results.

In this work, the Mercury problem was also studied in the SR Dynamics

framework with a remarkable conclusion that the effects is three times smaller than in GR and have an opposite sign. In other words, the orbital retardation rather than the advance takes place. Undoubtedly, GPS problem should be thoroughly studies in the SR Dynamics too.

10 The main claims, suggestions, conclusions

The results are finalized, as follows.

- The main goal of the work is the comparison of GR and Classical Dynamics predictions of the main characteristics of the Mercury's orbital motion in 3-space and time relevant to criteria of empirical verifications or falsification. An unambiguous formulation of comparison and required precisions of calculations and observations are made.
- There is a belief among physical "mainstream" community including GR workers that the Mercury's perihelion advance problem formulated by Einstein in November 1915 [1] has been fully studied and understood so that there were no issues to be considered anymore. We state, however, that it is wrong. In this work, it is shown that the problem has never been studied by finding full (angular and temporal) exact solutions to the GR equations of the test particle motion. Only such solutions reveal the role of dynamic structure of the GR curved 4-space.
- We suggest to abandon the geometrical orbital models in spherical symmetric geometry in favor of Physical parametrization for good reasons, in particular, to use minimal two independent parameters in relativistic theories in connections with the initial conditions. There, the σ parameter is actually expresses the Virial Theorem meaning an averaging potential and kinetic energies over time periods. This theorem can be principally generalized in relativistic models of "unclosed" orbits.
- The GR prediction of perihelion angular advance apart from a prediction of the corresponding GR temporal shift with respect to the classical picture is not sufficient for understanding the problem at the deeper level and formulating the criteria of a theoretical comparison of GR and classical theories.

- The disparity between GR and classical scales of dynamical variables such as time, angle, radius, and others cannot be ignored in the concept of empirical testing of Einstein's theory. Consequently, a usage of "approximations" related to the assumed equality of GR and Classical time would be flawed.
- The exact solutions of the GR particle motion in the whole range of field strength are conducted for the first time. They are also applicable to rigorous treatments of planetary motions as well Astrophysical and Cosmological observations. So far in literature, they are "explained" only in the approximate models.
- It is claimed that all quantitative results are correct and verifiable by calculations.
- The results confirm the existence of known controversial issues concerning both weak and strong field solutions, also reveal new questions. Consequently, the alternative approach to the GR particle dynamics is suggested and realizes in this work. The approach is based on the SR Dynamics methodology and basically consistent with the quantum field theories. It is concluded that old and new questions and problems do not arise there. For this reason, the Alternative (SR-based) Dynamics is additionally studied, which is claimed to be free of GR controversies, beyond that, suggesting new interpretations of strong field physical phenomena.
- We suggest to reconsider the current status of GR particle dynamics, allegedly, with "no questions left", including approximate methodologies of GR treatments of observations, and the criteria of GR verification/falsification. The criterion needs to account for full exact solutions of the problem. The questions are raised concerning unambiguous physical formulations of exact versus approximate solutions to be further studied.
- The presented ideas and findings are claimed to be novel and constructing, denying of which would be a discreditation of the real value of General Relativity theory for Astronomy and other applications.

This work is intended to draw the attention of researchers in General Relativity theory, as well as Astronomy, Astrophysics, Particle Physics, and

Cosmology, to our new results concerning the classical and relativistic gravitational theories in their comparison, and interpretations of non-classical effects in the whole range of field strength. Also, it can be interesting for Physical community, including workers in Mathematics and Philosophy of Natural sciences. It can be of pedagogical value as well. The author appreciate any critical comments, recommendations, and questions stimulating further discussions and studies.

11 References

[1] Albert Einstein. Erklärung der Perihelbewegung des Merkur aus der allgemeinen Relativitätstheorie. Sitzungsberichte der Königlich Preussischen Akademie der Wissenschaften zu Berlin, 1915. See also "The Collected Papers of Albert Einstein". vol. 6, Princeton University Press, (1996).

[2] Wolfgang Engelhardt. Free fall in gravitational theory. *Physics Essays*, 30(3):294–297, 2017.

[3] Anatoli Vankov. General Relativity Problem of Mercury's Perihelion Advance Revisited. arXiv:1008.1811 [physics.gen-ph], 2010.

[4] Kirill Vankov. The Problem of Particle Motion in the Schwarzschild Field: Critical Methodological Analysis, Exact Numerical Solution, and the Alternative. *The General Science Journal*, 2016.

[5] Kirill Vankov. General Relativity Mercury's Anomaly Prediction: What and How to Test? *The General Science Journal*, 2016.

[6] Yusuke Hagihara. Theory of the relativistic trajectories in a gravitational field of Schwarzschild. *Annales de l'Observatoire astronomique de Tokyo*, 31:67–176, 1931.

[7] Subrahmanyan Chandrasekhar. *The mathematical theory of black holes*, volume 69 of *International Series of Monographs on Physics*. Clarendon Press/Oxford University Press, New York/Oxford, 1983.

[8] Georgios Kraniotis and Steve Whitehouse. Compact calculation of the perihelion precession of Mercury in general relativity, the cosmological constant and Jacobi's inversion problem. *Classical and Quantum Gravity*, 20(22):4817, 2003.

[9] Karl Schwarzschild. On the Gravitational Field of a Mass Point According to Einstein's Theory. *General Relativity and Gravitation*, 35(5):951–959, 2003. Über das Gravitationsfeld eines Massenpunktes nach der Einsteinschen Theorie. Sitzungsberichte der Königlich Preussischen Akademie der Wissenschaften zu Berlin, Phys.-Math. Klasse 1916, 189–196.

[10] Peter Gabriel Bergmann. *Introduction to the Theory of Relativity*. Kessinger Publishing, 2008.

[11] Vladimir Fock. *The Theory of Space, Time and Gravitation*. Pergamon, 1959.

[12] Lev Davidovich Landau and Evgenii Mikhailovich Lifshitz. *The classical theory of fields*. Pergamon Press, Oxford, 1971.

[13] Yvonne Choquet-Bruhat. *General relativity and the Einstein equations*. Oxford University Press, 2009.

[14] Edmund Taylor Whittaker and George Neville Watson. *A Course of Modern Analysis*. Cambridge University Press, 1927.

[15] Richard Courant and Adolf Hurwitz. *Funktionentheorie*. Verlag von Julius Springer, Berlin, 1929.

[16] Claus Lämmerzahl. Testing Basic Laws of Gravitation–Are Our Postulates on Dynamics and Gravitation Supported by Experimental Evidence? In *Mass and Motion in General Relativity*, pages 25–65. Springer, 2011.

[17] Henri Cohen. *A course in computational algebraic number theory*, volume 138 of *Graduate Texts in Mathematics*. Springer, 1993.

[18] John Cremona. *Algorithms for modular elliptic curves*. Cambridge University Press, 1997.

[19] Jean-Benoît Bost and Jean-François Mestre. Moyenne arithmético-géométrique et périodes des courbes de genre 1 et 2. *Gaz. Math*, 38:36–64, 1988.

[20] John Cremona and Thotsaphon Thongjunthug. The complex AGM, periods of elliptic curves over C and complex elliptic logarithms. *Journal of Number Theory*, 133(8):2813–2841, 2013.

[21] W. A. Stein et al. *Sage Mathematics Software (Version 6.4)*. The Sage Development Team, 2014. `http://www.sagemath.org`.

[22] The PARI Group. *PARI/GP version 2.7.1*. Bordeaux, 2014. available from `http://pari.math.u-bordeaux.fr/`.

[23] Christian Møller. *The theory of relativity*. Clarendon Press, Oxford, 1972.

[24] Steven Weinberg. *Gravitation and cosmology: principles and applications of the general theory of relativity*. Wiley New York, 1972.

[25] Edwin F Taylor, John Archibald Wheeler, and Edmund William Bertschinger. *Exploring Black Holes: Introduction to General Relativity*. Addison-Wesley, 2010.

[26] Emmy Noether. Invariante Variationsprobleme. *Nachr. D. König. Gesellsch. D. Wiss. Zu Göttingen, Math-phys. Klasse*, (2):235–257, 1918.

[27] K.A. Olive and Particle Data Group. Review of Particle Physics. *Chinese Physics C*, 38(9):090001, 2014.

[28] U.S.NAVY. The Astronomical Almanac. Constants., 2017. Avaialable at `http://asa.usno.navy.mil/SecK/Constants.html`.

[29] NASA. Lunar and planetary science. Mercury fact sheet., 2016. See `http://nssdc.gsfc.nasa.gov/planetary/factsheet/mercuryfact.html`, accessed on 2017-08-03.

[30] Charles W. Misner, Kip S. Thorne, and John Archibald Wheeler. *Gravitation*. W. H. Freeman and Co, San Francisco, 1973.

[31] S. I. Blinnikov, L. B. Okun, and M. I. Vysotskii. Critical velocities $c/\sqrt{3}$ and $c/\sqrt{2}$ in the general theory of relativity. *Physics-Uspekhi*, 46(10):1099–1103, 2003.

[32] Anatoli Vankov. On Relativistic Generalization of Gravitational Force. *Foundations of Physics*, 38(6):523–545, 2008.

[33] John Lighton Synge. *Relativity: the special theory*. North Holland Publishing Company, Amsterdam, 1965.

[34] Netsivi Ben-Amots. A new line element derived from the variable rest mass in gravitational field. arXiv:0808.2609 [physics.gen-ph], 2008.

[35] Anatoli Vankov. Different Look at Relativistic Gravity and Related Phenomena. In Valeriy Dvoeglazov, editor, *Relativity, Gravitation, and Cosmology: New Developments*, Contemporary Fundamental Physics, pages 167–194. Nova Science Publishers, 2010.

[36] Jay Marx, Karsten Danzmann, James Hough, et al. The Gravitational Wave International Committee Roadmap: The future of gravitational wave astronomy. arXiv preprint arXiv:1111.5825, 2011.

[37] Leor Barack, Vitor Cardoso, Samaya Nissanke, et al. Black holes, gravitational waves and fundamental physics: a roadmap. arXiv preprint arXiv:1806.05195, 2018.

[38] Leor Barack and Adam Pound. Self-force and radiation reaction in general relativity. arXiv preprint arXiv:1805.10385, 2018.

[39] Luc Blanchet and Alexandre Le Tiec. First law of compact binary mechanics with gravitational-wave tails. *Classical and Quantum Gravity*, 34(16):164001, 2017.

[40] Gravitational Wave International Committee. The future of gravitational wave astronomy. `https://gwic.ligo.org/roadmap/`, Jun 2010.

[41] Jorge L. Cervantes-Cota, Galindo-Uribarri Salvador, and Smoot George F. A Brief History of Gravitational Waves. *Universe*, 2(3):22, 2016.

[42] David Blair, Li Ju, ChunNong Zhao, et al. Gravitational wave astronomy: the current status. *Science China Physics, Mechanics & Astronomy*, 58(12):120402, Dec 2015.

[43] Charles W Misner. Precis of general relativity. arXiv:gr-qc/9508043, 1995.

[44] Elliott Kaplan and Christopher Hegarty. *Understanding GPS: principles and applications*. Artech house, 2005.

[45] Neil Ashby. Relativity and the global positioning system. *Physics Today*, 55(5):41–47, 2002.

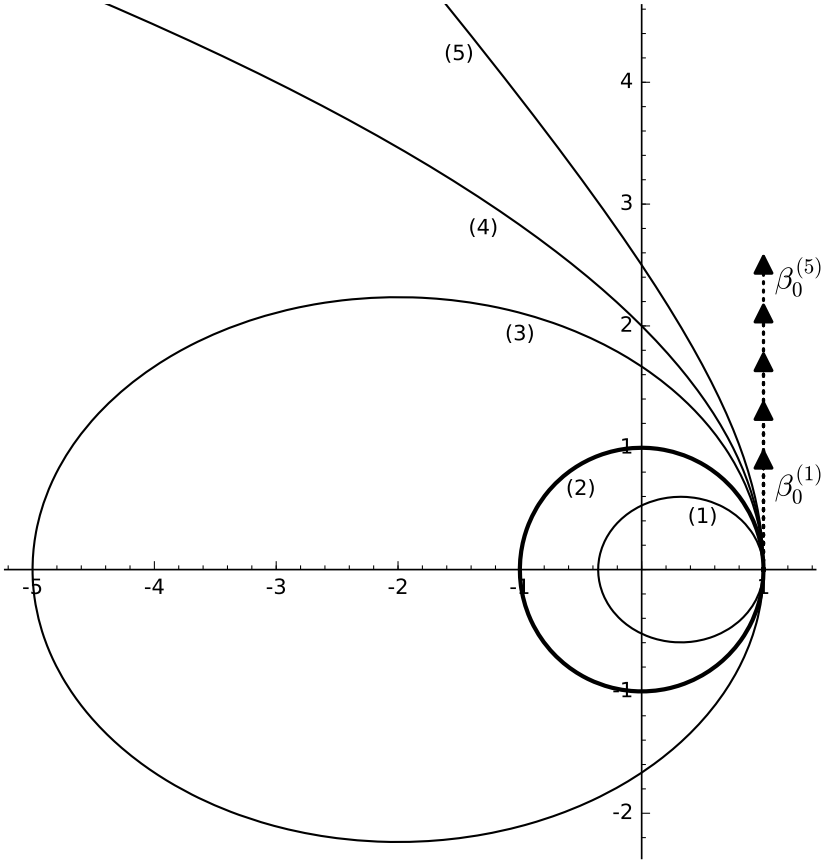

Figure 1: Classical orbits plotted in $(x,\ y)$ plane, $r = \sqrt{x^2 + y^2}$. Illustration of the σ family of orbits: (1) Sub-circle ellipse, $\sigma = 1.9$; (2) Circle, $\sigma = 1$; (3) Over-circle ellipse, $\sigma = 0.6$; (4) Parabola, $\sigma = 0.5$; (5) Hyperbola, $\sigma = 0.4$. The gravity center is placed at the coordinate origin, which is at rest with respect to the far-away stars (an inertial coordinate system). All orbits are produced by launching a test particle at the point $x_0 = 1$ with different initial speed $\beta_0 = \sqrt{r_g/\sigma}$, the arrow shows the geometry without value specification. The meaning of terms "subcircle" and "overcircle" follows from the the orbit classification, and is illustrated in the picture, see the text.

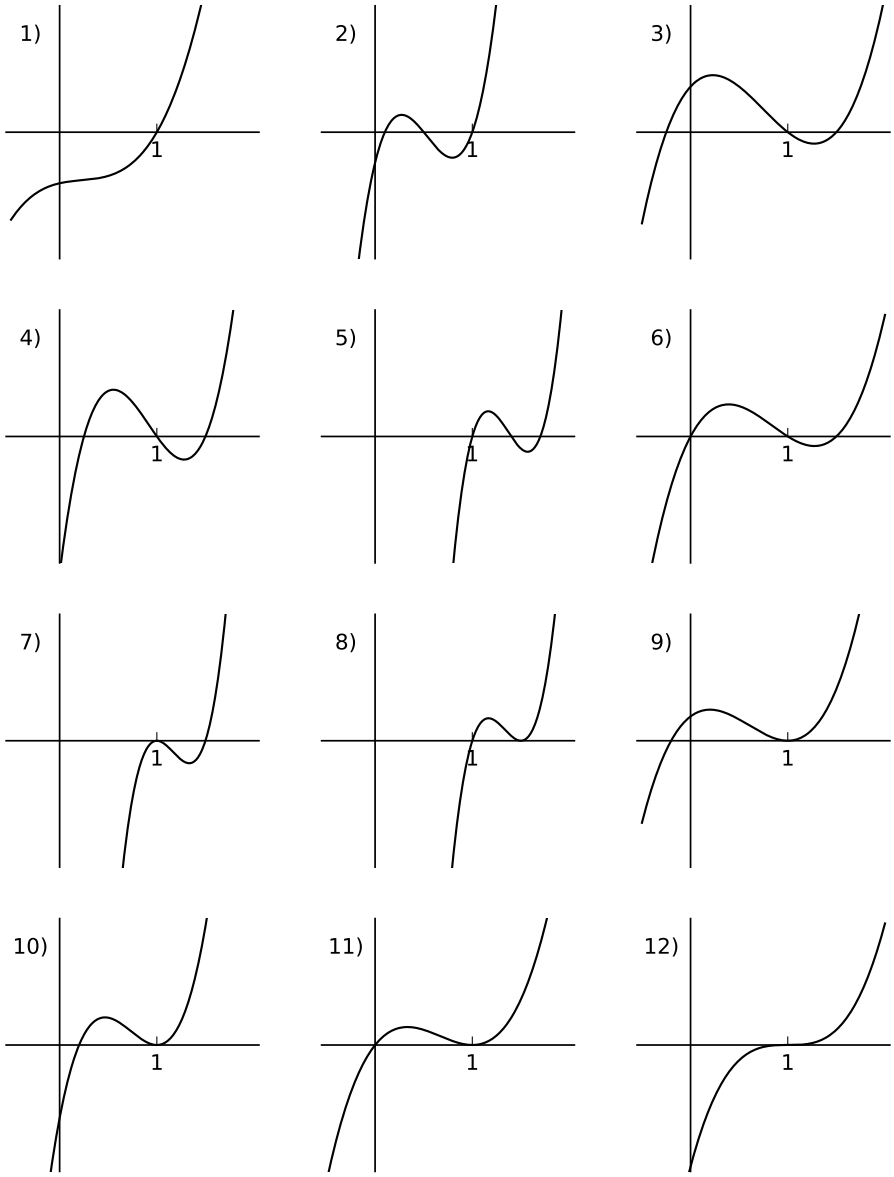

Figure 2: All possible roots of a cubic r.h.s. of (13):
1) complex ξ_2, ξ_3 roots; 2) $\xi_3 \leqslant \xi_2 < 1$; 3) $\xi_2 < 0$, $\xi_3 > 1$;
4) $0 < \xi_2 < 1$, $\xi_3 > 1$; 5) $1 < \xi_2 < \xi_3$; 6) $\xi_2 = 0$, $\xi_3 > 1$;
7) $\xi_2 = 1$, $\xi_3 > 1$; 8) $1 < \xi_2 = \xi_3$; 9) $\xi_2 < 0$, $\xi_3 = 1$;
10) $0 < \xi_2 < 1$, $\xi_3 = 1$; 11) $\xi_2 = 0$, $\xi_3 = 1$; 12) $\xi_2 = 1$, $\xi_3 = 1$.

Table 1: GR orbit classification: SF – spiral fall, H – hyperbola, P – parabola, C – circle, OC – over-circle, SC – sub-circle.

condition on ξ_2, ξ_3	relation between β_0^2 and ρ_0	orbit type	fig. 2
ξ_2, ξ_3 not real or $\xi_3 < 1$	$\rho_0 < \frac{1}{6}\,, \quad \beta_0^2 < \frac{16\,\rho_0^2}{1+4\,\rho_0-12\,\rho_0^2}$ or $\frac{1}{6} < \rho_0 < \frac{1}{3}\,, \quad \beta_0^2 < \frac{\rho_0}{1-3\rho_0}$ or $\rho_0 \geqslant \frac{1}{3}$	SF	1), 2)
$\xi_2 < 0$, $\xi_3 > 1$	$\rho_0 \leqslant \frac{1}{4}\,, \quad \beta_0^2 > \frac{2\rho_0}{1-2\rho_0}$ or $\frac{1}{4} < \rho_0 < \frac{1}{3}\,, \quad \beta_0^2 > \frac{\rho_0}{1-3\rho_0}$	H	3)
$\xi_2 < 1 < \xi_3$	$\rho_0 < \frac{1}{4}\,, \quad \frac{\rho_0}{1-3\,\rho_0} < \beta_0^2 < \frac{2\rho_0}{1-2\rho_0}$	OC	4)
$1 < \xi_2 < \xi_3$	$\rho_0 < \frac{1}{6}\,, \quad \frac{16\,\rho_0^2}{1+4\,\rho_0-12\,\rho_0^2} < \beta_0^2 < \frac{\rho_0}{1-3\rho_0}$	SC	5)
$\xi_2 = 0$, $\xi_3 > 1$	$\rho_0 < \frac{1}{4}\,, \quad \frac{2\rho_0}{1-2\rho_0}$	P	6)
$\xi_2 = 1$, $\xi_3 > 1$	$\rho_0 < \frac{1}{6}\,, \quad \beta_0^2 = \frac{\rho_0}{1-3\,\rho_0}$	C	7)
$1 < \xi_2 = \xi_3$	$\rho_0 < \frac{1}{6}\,, \quad \beta_0^2 = \frac{16\,\rho_0^2}{1+4\,\rho_0-12\,\rho_0^2}$	SC, SF	8)
$\xi_2 < 0$, $\xi_3 = 1$	$\frac{1}{4} < \rho_0 < \frac{1}{3}\,, \quad \beta_0^2 = \frac{\rho_0}{1-3\,\rho_0}$	H, C, SF	9)
$0 < \xi_2 < 1 = \xi_3$	$\frac{1}{6} < \rho_0 < \frac{1}{4}\,, \quad \beta_0^2 = \frac{\rho_0}{1-3\,\rho_0}$	OC, C, SF	10)
$\xi_2 = 0$, $\xi_3 = 1$	$\rho_0 = \frac{1}{4}\,, \quad \beta_0^2 = 1$	P, C, SF	11)
$\xi_2 = \xi_3 = 1$	$\rho_0 = \frac{1}{6}\,, \quad \beta_0^2 = \frac{1}{3}$	C, SF	12)

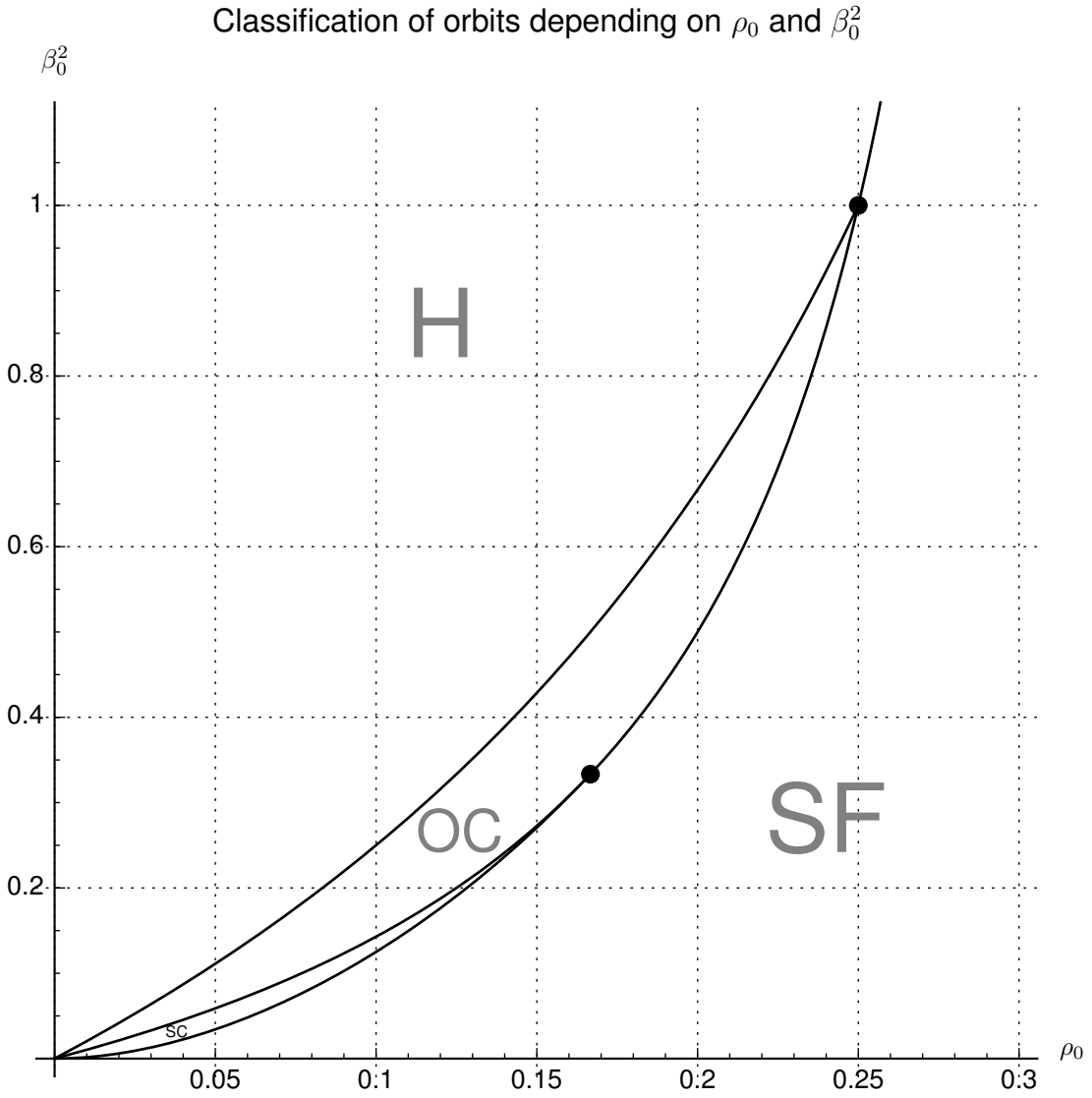

Figure 3: GR orbit classification on (ρ_0,β_0^2) plane: H – hyperbolic type; OC – over-circular type; SC – sub-circular type; SF – spiral fall type; parabolic type – line next to H; circular orbits – middle curve from 0 till $\rho_0 = 1/6$ continuing to $\rho_0 = 1/4$.

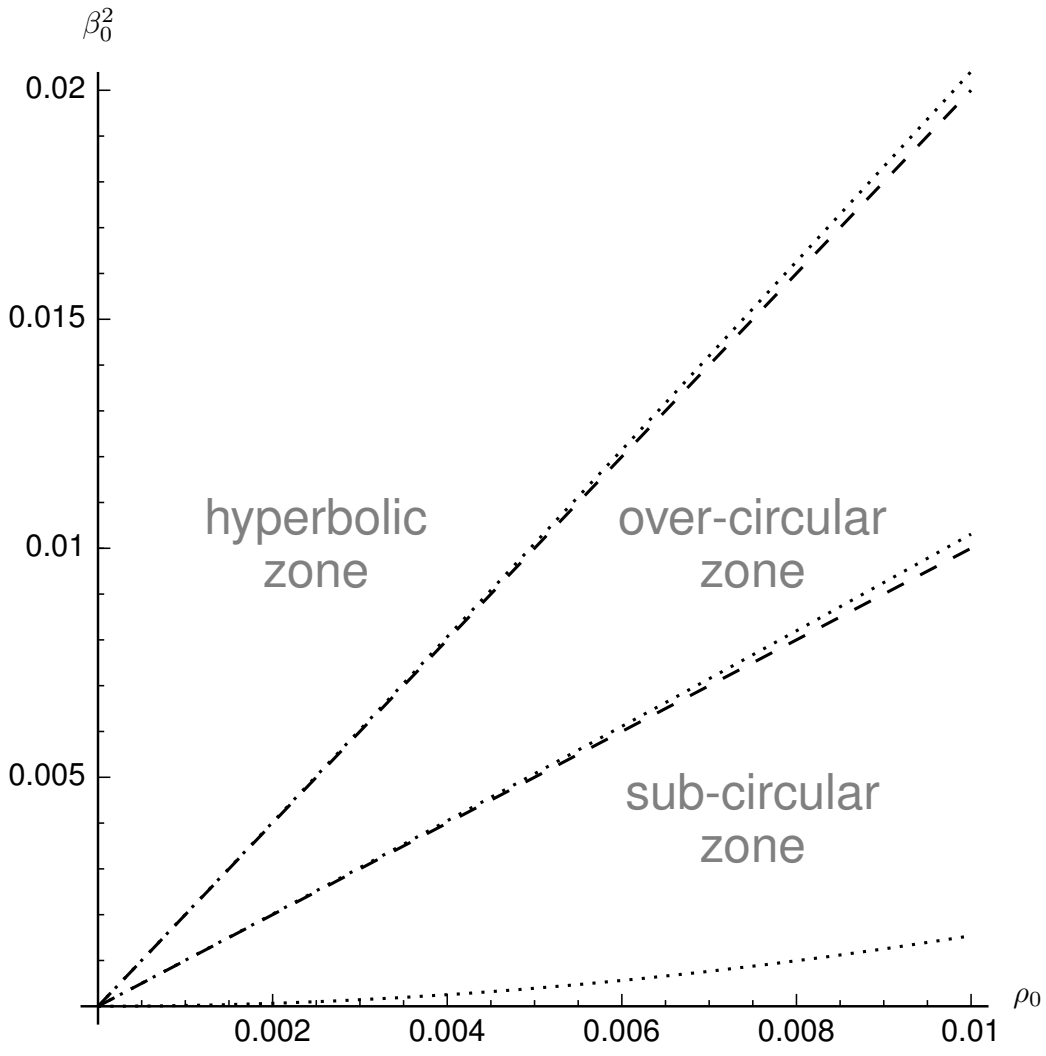

Figure 4: Orbit classification in classical mechanics (dashed lines): the top region corresponds to hyperbolic orbits, the top dashed line – parabolic orbits, in between the dashed lines – over-circular orbits, the bottom dashed line – circular orbits, below – sub-circular orbits. In GR theory (dotted curves) there is an additional (at the very bottom, below the dotted line) region with spiral-fall type of orbits. When ρ_0 and β_0^2 are small, the orbit classification in classical mechanics becomes similar to that in GR.

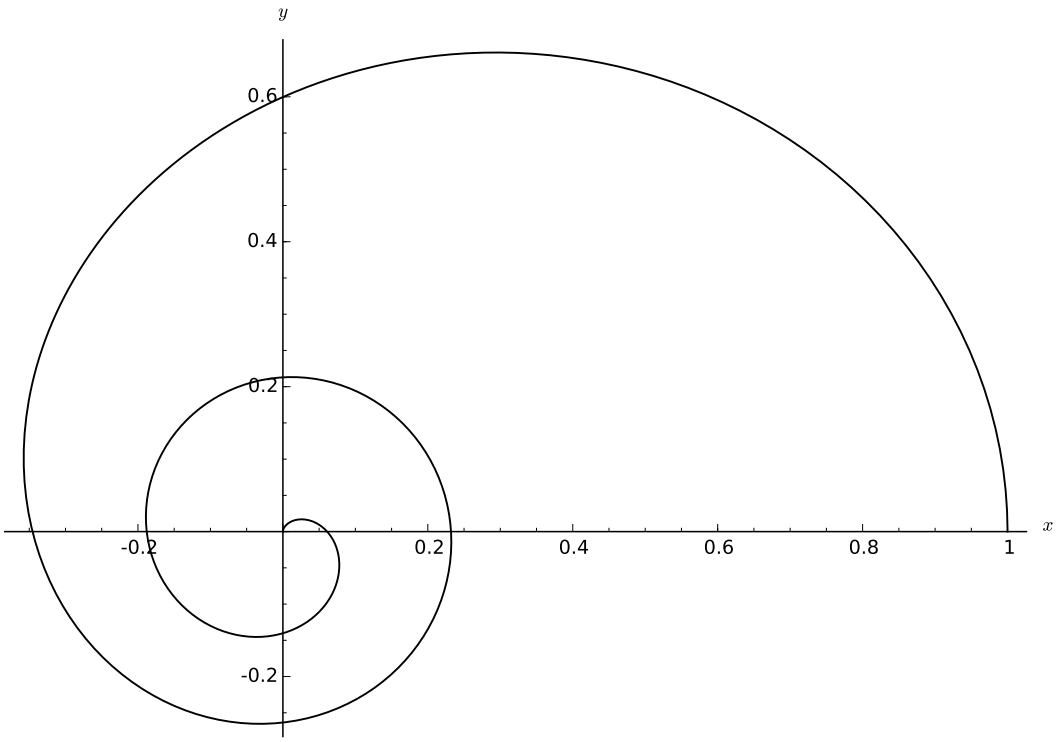

Figure 5: Spiral fall trajectory for $\rho_0 = 0.05$, $\beta_0^2 = 0.03$. Shown only half period.

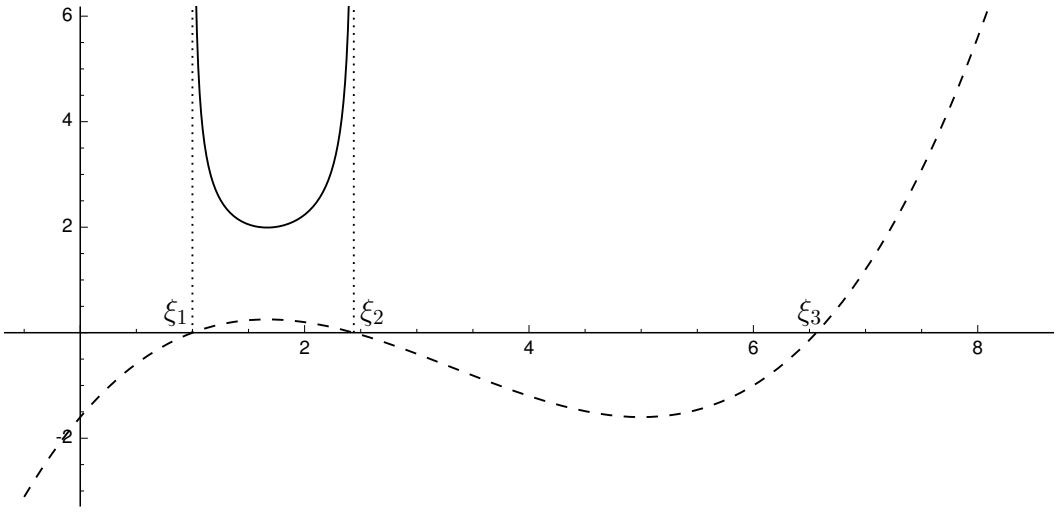

Figure 6: Typical case of polynomial $f(\xi)$ with three roots (here $\rho_0 = 0.05$, $\beta_0 = 0.04$, the dashed line). The integration is performed from $\xi_1 = 1$ to ξ_2 under the solid line.

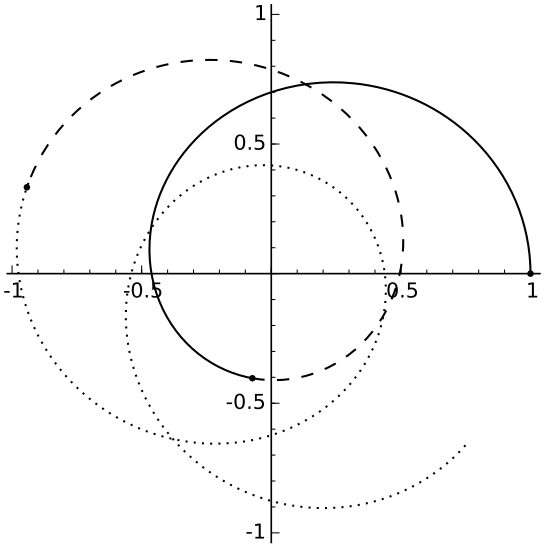

Figure 7: Orbit for $\rho_0 = 0.05$ and $\beta_0 = 0.04$. Starting point (1,0), following solid line first periapsis at point (0.41,4.53), following dashed line first period completed at point (1,9.07), continuing by dotted line for another period. All points are given in polar coordinates.

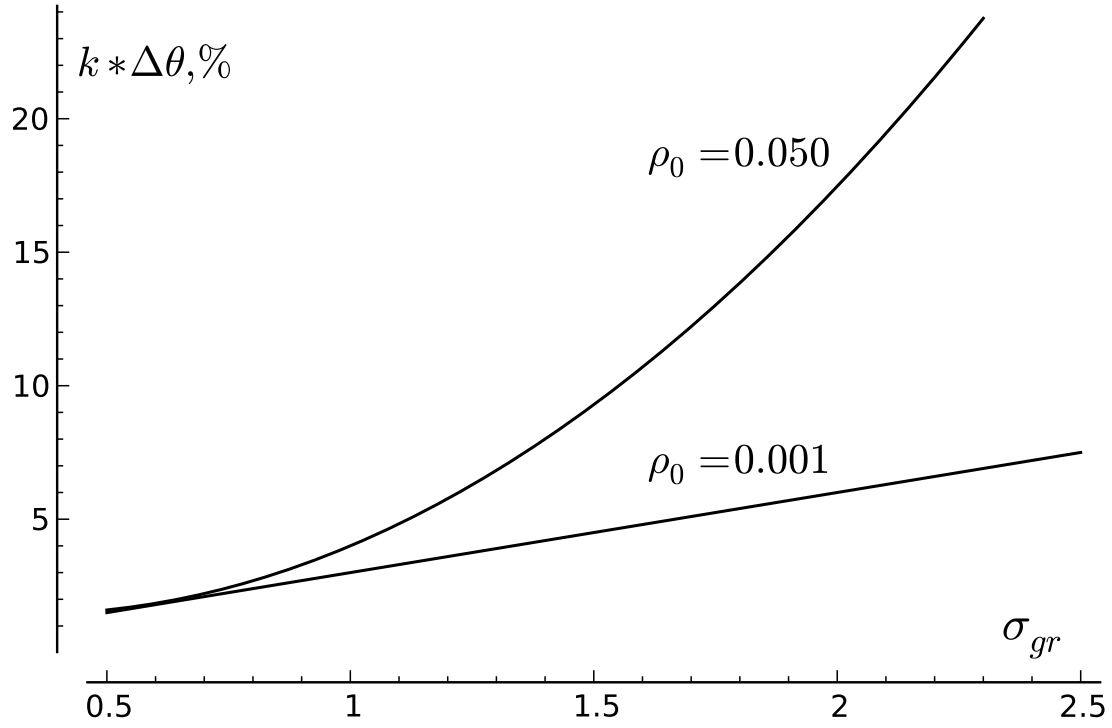

Figure 8: Dependence $\Delta\theta = 3\,\rho_0\,\sigma_{gr}$ of relative precessional advance on σ_{gr} as ρ_0 varies (exact numerical integration). Two curves are normalized to the same vertical plotting scale. Normalization coefficient $k = 10$ for $\rho_0 = 0.001$ (weak-field), and $k = 1/5$ for $\rho_0 = 0.050$ (mildly strong field) so that all lines for $\rho_0 < 0.001$ with proportionally however smaller effect coincide with the line for $\rho_0 = 0.001$. Deviated curves appear as the field strength rises with $\rho_0 > 0.001$.

Input parameters from the initial conditions:			
dimensionless $\rho_0 = r_g/r_0$	3.21×10^{-8}		
dimensionless β_0^2	3.87×10^{-8}		
dimensionless r_0	1		
Scaling quantities:			
The speed of light c	299792458 m/s		
Sun's standard gravitational parameter $\mu_0 = r_g c^2$	$1.32712440041\times10^{20}$ m^3/s^2		
Perihelion $r_0 = r_p$	4.6×10^{10} m		
Velocity at perihelion	58976 m/s		
Output:			
Computed characteristics	Classical theory q_{cl}	Absolute difference $q_{gr} - q_{cl}$	Relative difference $q_{gr}/q_{cl} - 1$
Aphelion radius r_a	69811764705.882 m	-14237.080 m	-2.039×10^{-7}
Velocity at aphelion	38860.233 m/s	7.924×10^{-3} m/s	2.039×10^{-7}
Angular full period	$2\,\pi$ rad	5.019×10^{-7} rad	7.988×10^{-8}
Time full period	7599967.916 s	-1.111 s	-1.461×10^{-7}
Full period orbit length	3.600×10^{11} m	-12603.073 m	-3.501×10^{-8}

Table 2: General comparison of the input and output results for Mercury in GR vs classical mechanics. In the input, we fixed perihelion and velocity at perihelion as well as the gravitational field strength in the initial conditions, which chosen common for the GR and the classical theory. The output includes the main exactly calculated values of classical characteristics q_{cl} of the orbit, also the absolute differences of the corresponding GR values $q_{gr} - q_{cl}$ and the relative differences $q_{gr}/q_{cl} - 1$ with respect to the classical values.

	Event 1: at $\theta_{gr} = \pi$	Event 2: GR aphelion	Event 3: $\tau_3 = t_2$
τ	3799982.951801 s	3799983.402610 s	3799983.957976 s
r_{gr}	69811750468.802 m	69811750468.802 m	69811750468.801 m
θ_{gr}	$\pi = 3.141592654$ rad	$pi + 2.509 \times 10^{-7}$ rad	$\pi + 5.600 \times 10^{-7}$ rad
v_{gr}	38860.241 m/s	38860.241 m/s	38860.241 m/s
l_{gr}	179978550169.643 m	179978567688.220 m	179978589269.852 m
t	3799983.507166 s	3799983.957976 s	3799984.513341 s
r_{cl}	69811764705.882 m	69811764705.882 m	69811764705.881 m
θ_{cl}	$\pi - 2.509 \times 10^{-7}$ rad	$\pi = 3.141592653$ rad	$\pi + 3.091 \times 10^{-7}$ rad
v_{cl}	38860.233 m/s	38860.233 m/s	38860.233 m/s
l_{cl}	179978556471.180 m	179978573989.757 m	179978595571.387 m
Absolute differences of GR and classical theory values			
$\tau - t$	-0.555365 s	-0.555365 s	-0.555365 s
$r_{gr} - r_{cl}$	-14237.080 m	-14237.080 m	-14237.080 m
$\theta_{gr} - \theta_{cl}$	2.509×10^{-7} rad	2.509×10^{-7} rad	2.509×10^{-7} rad
$v_{gr} - v_{cl}$	0.007925 m/s	0.007925 m/s	0.007925 m/s
$l_{gr} - l_{cl}$	-6301.538 m	-6301.537 m	-6301.535 m
Relative differences of GR with respect to classical values			
$(\tau - t)/t$	-1.461×10^{-7}	-1.461×10^{-7}	-1.461×10^{-7}
Δr	-2.039×10^{-7}	-2.039×10^{-7}	-2.039×10^{-7}
$\Delta\theta$	7.988×10^{-8}	7.988×10^{-8}	7.988×10^{-8}
Δv	2.039×10^{-7}	2.039×10^{-7}	2.039×10^{-7}
Δl	-3.501×10^{-8}	-3.501×10^{-8}	-3.501×10^{-8}

Table 3: Three-events comparison between classical theory and General Relativity theory. Shown are the absolute values of main orbital characteristics at events 1, 2, 3, predicted in each theory, including the time τ, t, the radius r_{gr}, r_{cl}, the angle θ_{gr}, θ_{cl}, the full orbital speed v_{gr}, v_{cl}, and the passed length along orbital trajectory l_{gr}, l_{cl}. Here and in the next tables, they are calculated in the first half-period starting from the initial conditions. The corresponding absolute values $q_{gr} - q_{cl}$ and relative differences of GR values with respect to classical ones $q_{gr}/q_{cl} - 1$ are also given. To the precision of 4 significant digits, differences do not change over the time interval, which includes the three events.

	classical theory	**GR**
Difference of values at event 2 and event 1		
time	0.450810 s	0.450810 s
radius	5.689×10^{-4} m	5.689×10^{-4} m
polar angle	2.509×10^{-7} rad	2.509×10^{-7} rad
full speed	-4.002×10^{-10} m/s	-3.986×10^{-10} m/s
trajectory length	17518.577 m	17518.578 m
Difference of values at event 3 and event 2		
time	0.555365 s	0.555365 s
radius	-8.634×10^{-4} m	-8.634×10^{-4} m
polar angle	3.091×10^{-7} rad	3.091×10^{-7} rad
full speed	6.039×10^{-10} m/s	6.050×10^{-10} m/s
trajectory length	21581.630 m	21581.631 m
Difference of values at event 3 and event 1		
time	1.006175 s	1.006175 s
radius	-2.945×10^{-4} m	-2.945×10^{-4} m
polar angle	5.601×10^{-7} rad	5.601×10^{-7} rad
full speed	2.064×10^{-10} m/s	2.064×10^{-10} m/s
trajectory length	39100.207 m	39100.209 m

Table 4: Three-events comparison between classical theory and General Relativity theory. Shown are the absolute differences of values of main orbital characteristics at events 1, 2, 3, predicted in each theory, including the time, the angle, the radius, the particle orbital speed, and the passed length, starting from the common initial conditions. They do not change in 4 significant numbers.

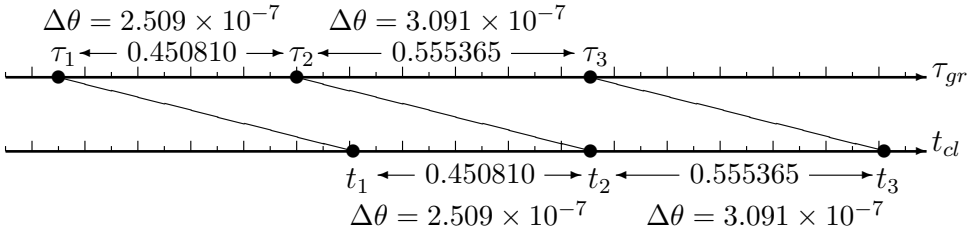

Table 5: Projections of GR three events to the classical time line. This is an illustration of the fact that the GR angular advance $\Delta\theta = 2.509 \times 10^{-7}$ rad and the temporal advance $\Delta\tau = 0.555$ s are caused by the common reason, – the cubic term in GR dynamics equations. The effects on the classical time line delay. In both theories, the time shift is formed between events (3, 2), while the GR angular shift between the events (2, 1) in half periods. The plot makes clear that "the approximation" of equality of GR and classical periods would mean a disappearance of the angular advance that is, flawed.

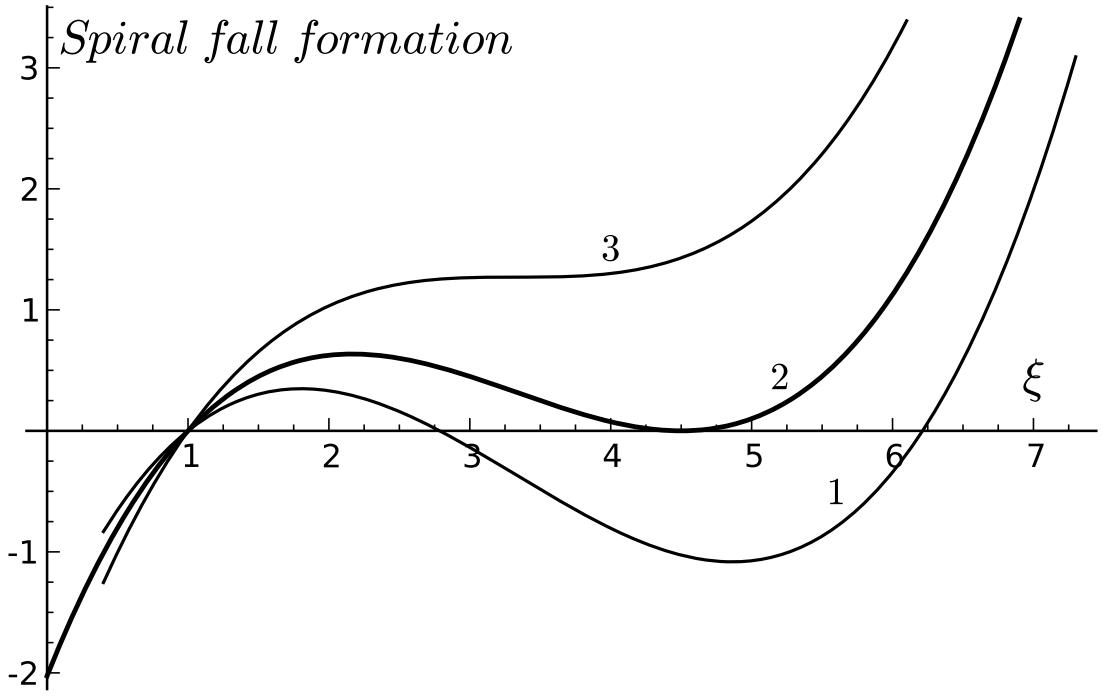

Figure 9: Plotted $f(\xi)$ (see text) for $\rho_0 = 0.050$. The curve 2 shows the edge point $\xi_2 = \xi_3 = 4.5$, with initial squared velocity $\beta^2_{edge} = 0.0341880$. The curve 1 is a sub-circle orbit with $\beta^2_0 = 0.038$. The curve 3 is an over-edge orbit, with $\beta^2_0 = 0.030$ and it illustrates the spiral fall trajectory that begins with $\beta^2_0 < \beta^2_{edge}$, when the roots ξ_2 and ξ_3 become complex.

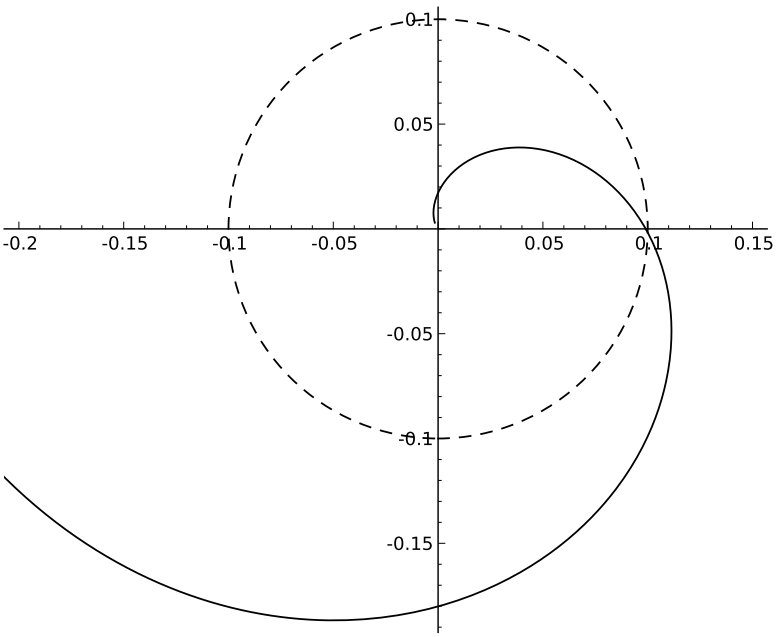

Figure 10: Spiral fall onto the center: crossing the Schwarzschild surface ($\xi = 10$, $r = 0.10$, $r_0 = 1$) in an over-edge orbit, $\rho_0 = 0.0500$, $\beta_0^2 = 0.300$, the case 3) in fig. 9. This figure shows proximity of a spiral sharp-dive onto the point center $r = 0$. The trajectory shown from some point before crossing of the Schwarzschild surface (dashed line). A particle crosses the Schwarzschild surface at the speed $\beta_{sch} = 1.982$, and, as shown in the picture, ended up deep inside the Schwarzschild sphere, at $r = r_g/15$ ($\xi = 300$), having a speed $\beta(1/300) = 285$.

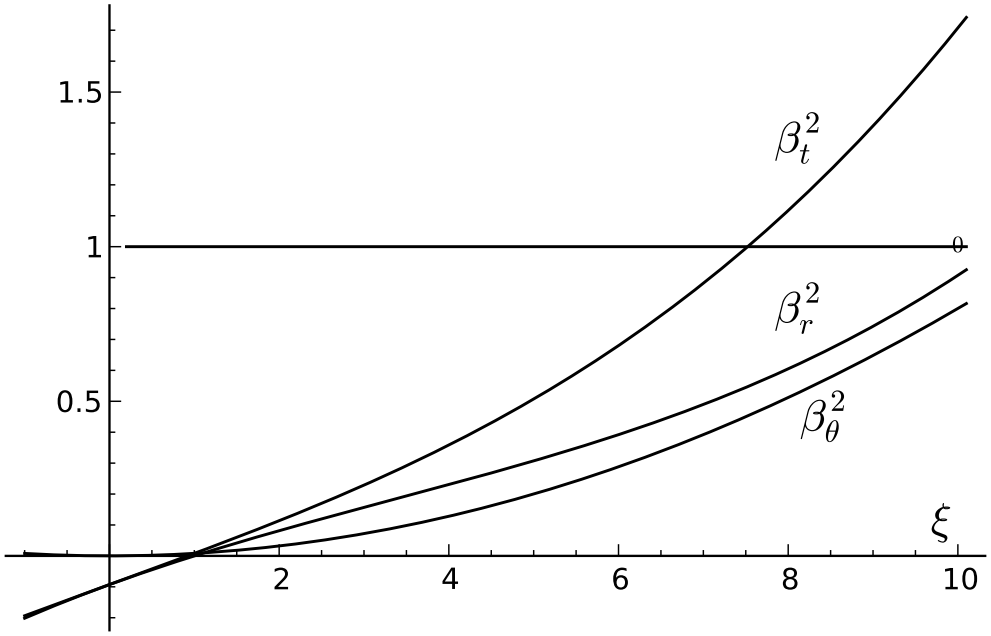

Figure 11: Example of over-edge motion: a spiral fall onto the center; $\rho_0 = 0.050$, $\beta_0^2 = 0.008$. Shown squared relative velocities of the test particle $\beta_r^2(\xi)$ (9), $\beta_\theta^2(\xi)$ (10), $\beta^2(\xi)$ (41); a conserved (squared) total energy $\epsilon_0^2 = 0.907$ (that is, a bounded motion). The particle crosses the Schwarzschild surface $\xi_{sch} = 10$ ($r_{sch} = 0.10$) at the resultant speed $\beta = 1.304$ (faster than light) with the kinetic energy $\beta_r^2 = 0.907$. The angular component of speed is $\beta_\theta^2 = 0.800$ (in this example, it is less than the speed of light), and the resultant one $\beta^2 = 1.707$ (faster than light). The particle reaches the resultant speed equal to the speed of light $\beta = 1$ at the radial point $\xi = 7.54$ ($r = 0.133$), that is outside the interior region.

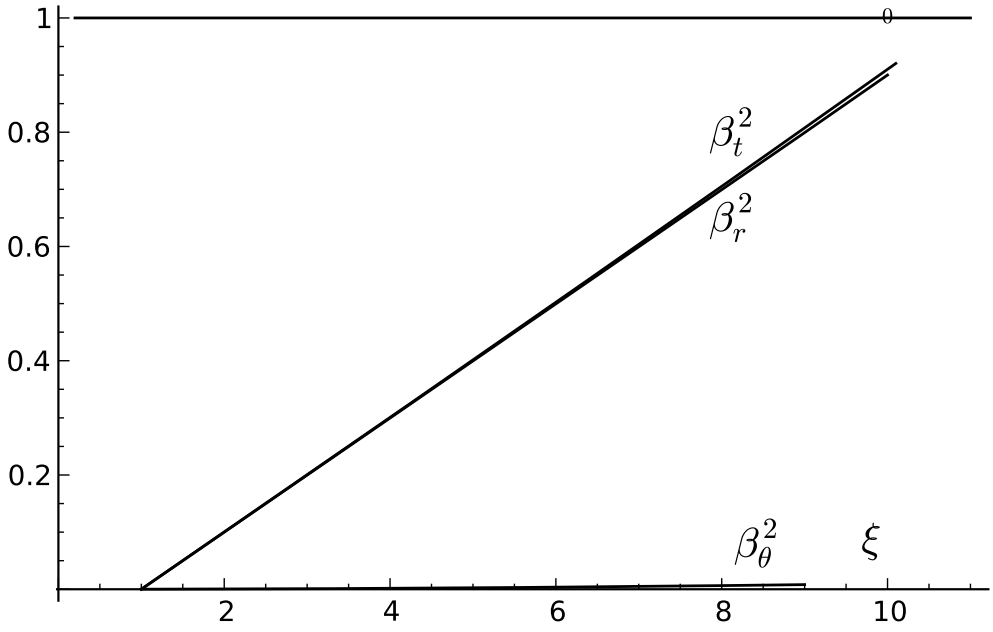

Figure 12: The case of subluminal motion: spiral fall onto the center; $\rho_0 = 0.050$, $\beta_0^2 = 0.0001$. Shown squared relative velocity components $\beta_r^2(\xi)$ (9), $\beta_\theta^2(\xi)$ (10), $\beta_t^2(\xi)$ (41); a conserved (squared) total energy $\epsilon_0^2 = 0.900$. The particle crosses the horizon at the resultant speed $\beta_t = 0.910$ (less than speed of light) with velocity (squared) components $\beta_r^2 = 0.900$, $\beta_\theta^2 = 0.010$.

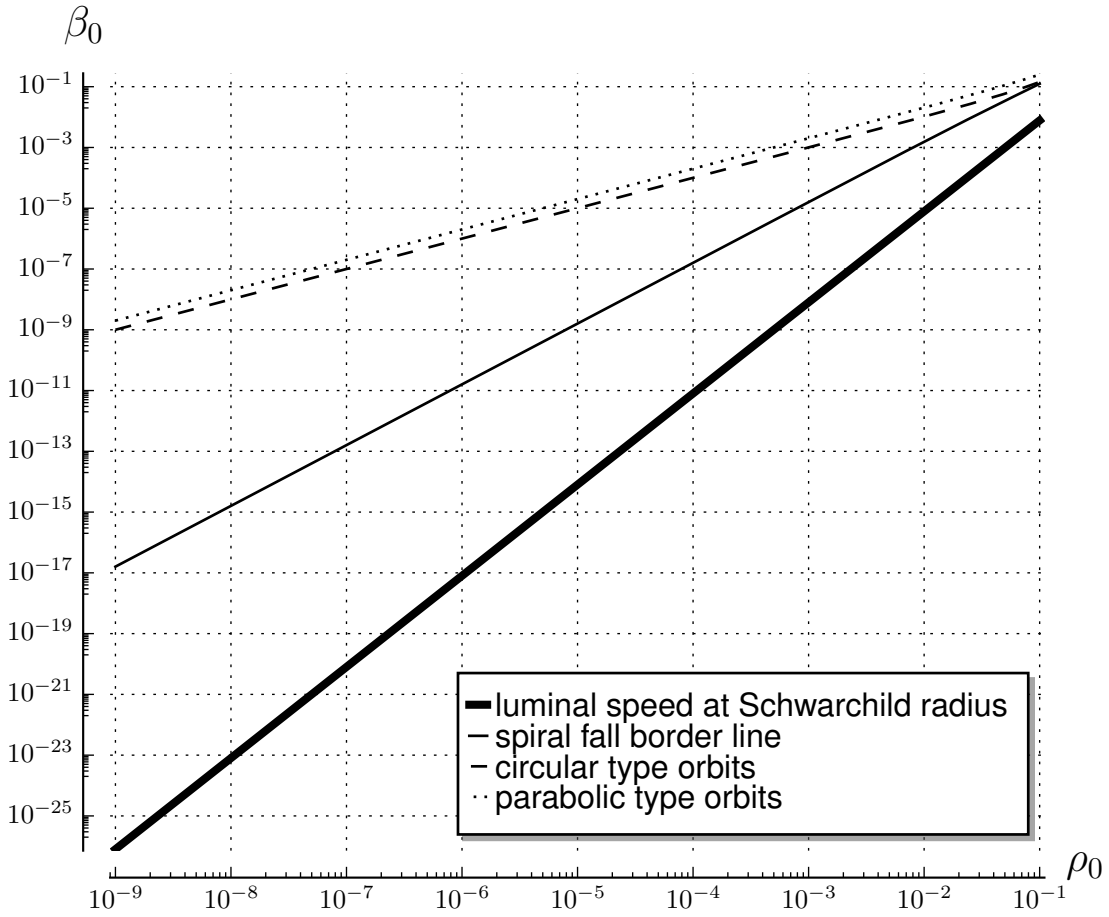

Figure 13: Conditions of the luminal speed at Schwarzschild radius. For the values (ρ_0, β_0^2) below the thick line the full speed of a particle at Schwarzschild radius is lower than the speed of light, between the thick and the solid lines, the speed is greater than the speed of light.

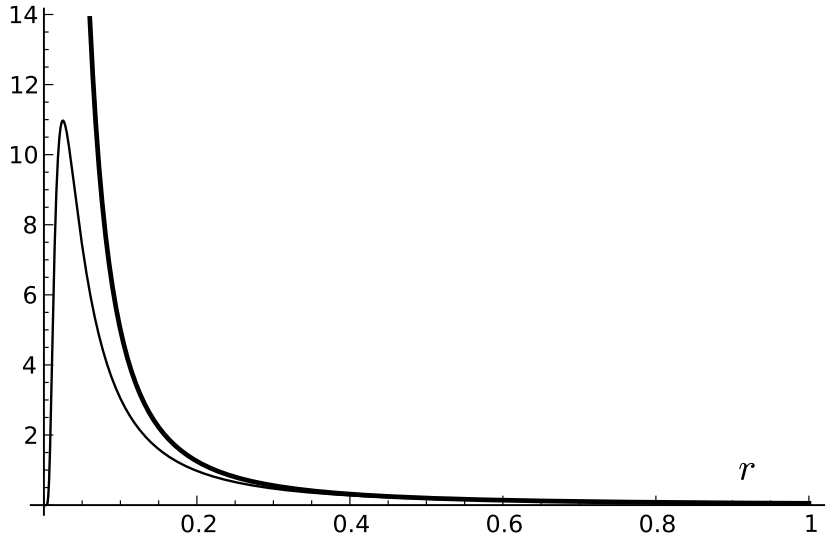

Figure 14: Newtonian attractive force $F(r) \sim r_g/r^2$ (thick line) and its relativistic generalization $F_R(r) \sim r_g/r^2 \exp(-r_g/r)$ in the concept of field-dependent proper mass, in the example of a strong interaction $r_g = 0.05$. It has a maximal absolute value at $r = r_g$, and $F_R(r) \to 0$ as $r \to 0$; in the range $r < r_g$, it rises with distance and asymptotically $F_R(r) \to F(r)$ as $r \to \infty$.

Input parameters:			
dimensionless $\rho_0 = r_g/c^2$	3.21×10^{-8}		
dimensionless β_0^2	3.87×10^{-8}		
dimensionless r_0	1		
Scaling quantities:			
The speed of light c	299792458 m/s		
Sun standard gravitational parameter $\mu_0 = r_g c^2$	$1.32712440041\times10^{20}$ m^3/s^2		
Perihelion r_p	4.6×10^{10} m		
Velocity at perihelion	58976 m/s		
Output:			
Computed characteristics	Classical theory q_{cl}	Absolute difference Δq	relative difference δq
Aphelion r_a	69811764705.882 m	4877.583 m	6.987×10^{-8}
Velocity at aphelion	38860.233 m/s	-2.715×10^{-3} m/s	-6.986×10^{-8}
Angular full period	$2\,\pi$ rad	-1.673×10^{-7} rad	-2.663×10^{-8}
Time full period T	7599967.916 s	0.383 s	5.042×10^{-8}
Full period orbit length	3.600×10^{11} m	4510.132 m	1.253×10^{-8}

Table 6: The input and output data for computing Mercury's orbital characteristics in Classical and SR Dynamics are shown. In the input, there are only two independent model parameters, ρ_0 and β_0^2, from the initial conditions common for both theories. In the output, absolute values of main classical characteristics q_{cl} integrated over the full period, and their absolute and relative differences $\Delta q = q_{sr} - q_{cl}$, $\delta q = q_{sr}/q_{cl} - 1$ with respect to corresponding Classical Dynamics, are given.

	Event 1: $t_{sr}(1) = t_{cl}(2)$	Event 2 SR aphelion	Event 3: SR $\theta = \pi$
t_{sr}	3799983.957976 s	3799984.149588 s	3799984.299859 s
r_{sr}	69811769583.465 m	69811769583.465 m	69811769583.465 m
θ_{srd}	$\pi - 1.903 \times 10^{-7}$ rad	$\pi - 8.364 \times 10^{-8}$ rad	$\pi = 3.141592653$ rad
v_{sr}	38860.230 m/s	38860.230 m/s	38860.230 m/s
l_{sr}	179978568798.694 m	179978576244.823 m	179978582084.349 m
t_{cl}	3799983.766362 s	3799983.957976 s	3799984.108246 s
r_{cl}	69811764705.882 m	69811764705.882 m	69811764705.882 m
θ_{cl}	$\pi - 1.066 \times 10^{-7}$ rad	$\pi = 3.141592653$ rad	$\pi + 8.364 \times 10^{-8}$ rad
v_{cl}	38860.233 m/s	38860.233 m/s	38860.233 m/s
l_{cl}	179978566543.628 m	179978573989.757 m	179978579829.283 m
Absolute differences between SRD and classical theories			
Δt	0.191613 s	0.191613 s	0.191613 s
Δr	4877.583 m	4877.583 m	4877.583 m
$\Delta\theta$	-8.365×10^{-8} rad	-8.365×10^{-8} rad	-8.365×10^{-8} rad
Δv	-0.002715 m/s	-0.002715 m/s	-0.002715 m/s
Δl	2255.066 m	2255.066 m	2255.066 m
Relative differences between SRD and classical theories			
δt	5.042×10^{-8}	5.042×10^{-8}	5.042×10^{-8}
δr	6.987×10^{-8}	6.987×10^{-8}	6.987×10^{-8}
$\delta\theta$	-2.663×10^{-8}	-2.663×10^{-8}	-2.663×10^{-8}
δv	-6.987×10^{-8}	-6.987×10^{-8}	-6.987×10^{-8}
δl	1.253×10^{-8}	1.253×10^{-8}	1.253×10^{-8}

Table 7: Orbital Mercury's characteristics q_{sr} computed at 3 events in SR Dynamics time scale t_{sr} in comparison with q_{cl} computed in the classical time scale t_{cl} starting with the common initial conditions are shown. Also shown their absolute and relative differences $\Delta q = q_{sr} - q_{cl}$, $\delta q = q_{sr}/q_{cl} - 1$. The following characteristics are computed at each event: the time passed t_{sr}, t_{cl}, the radius r_{sr}, r_{cl}, the orbital angle θ_{sr}, θ_{cl}, the orbital speed v_{sr}, v_{cl}, the orbital length l_{sr}, l_{cl}.

	Classical theory	**SR theory**
Difference between Event 2 and Event 1		
Time	0.191613 s	0.191613 s
Radius	1.028×10^{-4} m	1.028×10^{-4} m
Polar angle	1.067×10^{-7} rad	1.067×10^{-7} rad
Full speed	-7.276×10^{-11} m/s	-7.202×10^{-11} m/s
Trajectory length	7446.129 m	7446.129 m
Difference between Event 3 and Event 2		
Time	0.150270 s	0.150270 s
Radius	-6.321×10^{-5} m	-6.321×10^{-5} m
Polar angle	8.365×10^{-8} rad	8.365×10^{-8} rad
Full speed	4.366×10^{-11} m/s	4.429×10^{-11} m/s
Trajectory length	5839.526 m	5839.526 m
Difference between Event 3 and Event 1		
Time	0.341883 s	0.341883 s
Radius	3.957×10^{-5} m	3.957×10^{-5} m
Polar angle	1.903×10^{-7} rad	1.903×10^{-7} rad
Full speed	-2.773×10^{-11} m/s	-2.773×10^{-11} m/s
Trajectory length	13285.655 m	13285.654 m

Table 8: Absolute differences of orbital characteristics between events (2, 1), (3, 2), (3, 1) computed in SR Dynamics and Classical theory.

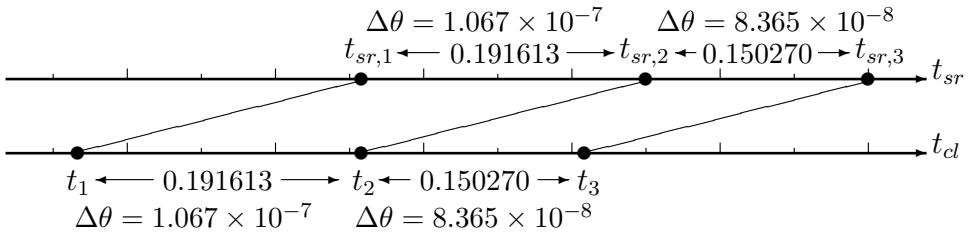

Table 9: The projections of the three SR events on the base time line t_{sr} and the classical time line t_{cl} are shown, which, again, demonstrate the disparity of angular and temporal shifts on the uniform time scales. The retardation of SR time clock and angular shift, as opposed to the GR advance, is demonstrated. It makes a tremendous positive impact on SR Physics of orbits, see the text